

# $W$ mass and Leptonic $Z$ -decays in the NMSSM

Florian Domingo\* and Teresa Lenz

*Institut für Theoretische Teilchenphysik  
Karlsruher Institut für Technologie (Universität Karlsruhe)  
D-76128 Karlsruhe, Germany*

## Abstract

We study a subset of electroweak-precision observables consisting of  $M_W$ ,  $\sin^2 \theta_{\text{eff}}^\tau$ ,  $BR(Z \rightarrow \tau^+ \tau^-)$  and  $\Gamma(Z \rightarrow \tau^+ \tau^-)/\Gamma(Z \rightarrow e^+ e^-) - 1$  (characterizing leptonic  $Z$ -decays) in the context of the NMSSM. After a brief review of common MSSM-NMSSM effects (*e.g.* for  $\Gamma(Z \rightarrow \tau^+ \tau^-)/\Gamma(Z \rightarrow e^+ e^-) - 1$ , which has been little discussed, even in the MSSM), specific NMSSM scenarios are studied, with the result that the NMSSM, considering existing constraints on its spectrum, is essentially consistent with available measurements, given the current accuracy.

## 1 Introduction

ElectroWeak Precision Observables (EWPOs) [1] are sensitive to quantum corrections and thus to possible new physics effects. They are very accurately measured: current experimental data from LEP, SLD [2] or TeVatron [3] reach percent-level accuracy. Future improvements are expected from LHC [4] and, in a more distant future, from a possible ILC with GigaZ option [5]. Such a high level of precision makes these EWPOs useful to probe the Standard Model (SM) and its extensions, and constrain, provided the same accuracy can be matched on the theoretical side, the parameter spaces of such models. They are, in any case, unavoidable tests of the electroweak symmetry-breaking sector.

In the SM, the EWPOs are currently used to constrain the only unknown free parameter, *i.e.* the Higgs mass, leading to the result  $M_H^{SM} = 76_{-44}^{+33}$  GeV ( $M_H^{SM} \leq 144$  GeV at 95% confidence level) [6] (see also [2, 3]). One observes the slight tension between this range and the current experimental lower bound on  $M_H^{SM}$ , resulting from direct searches at LEP ( $M_H^{SM} \gtrsim 114$  GeV) [7]. Beyond the SM, its simplest (softly-broken) supersymmetric extension, the MSSM, was already thoroughly investigated under the light of EWPOs (see [8–10] for comprehensive reviews on the subject): several new contributions are expected, both from the extended Higgs sector and from the supersymmetric sector. Yet, a preference for rather light SUSY spectra (in the mSUGRA version of the MSSM) has been noted [11], while, on the other hand, sensibly heavy SUSY particles are required to generate sufficiently large corrections to the lightest Higgs mass (in order to circumvent the experimental lower bound) [12].

In the following, we will focus on the popular singlet ( $\mathbb{Z}_3$ -invariant, minimally CP and flavour-violating) extension of the MSSM, known as the Next-to-Minimal Supersymmetric Standard Model (NMSSM; see [13] for a review and standard notations for NMSSM parameters). The leading motivation behind this singlet extension lies in solving the  $\mu$ -problem of the MSSM [14]. Moreover, several remarkable Higgs scenarii are known to be viable in the NMSSM, resulting in *e.g.* possibly light CP-even states  $h_1$ , either dominantly singlet (hence having reduced coupling to the SM sector) [15] or decaying unconventionally into light CP-odd Higgs  $A_1$  below the  $B - \bar{B}$  threshold (see *e.g.* [16]). This last possibility has been further constrained by a new-analysis of ALEPH data [17]. Nevertheless, reduced branching ratios of the  $A_1$  into  $\tau^+ \tau^-$ , according to [18], or increased singlet components of the  $h_1$ , may still be consistent with experimental limits. Significant interest was dedicated to  $m_{h_1} \sim 98$  GeV [19], where, in virtue of its reduced couplings or its unconventional decays, a NMSSM CP-even Higgs could explain the small excess ( $2.3\sigma$ ) observed at LEP in the channel

---

\*email: domingo@particle.uni-karlsruhe.de

$e^+e^- \rightarrow Z + b\bar{b}$  [12]. Note also that, independently of the CP-even Higgs (with  $h_1$  possibly as heavy as  $\sim 140$  GeV in the NMSSM), light CP-odd Higgs represent another original NMSSM possibility with respect to the MSSM and may be natural in a R or Peccei-Quinn symmetry limit of the parameter space. Other NMSSM-specific effects are known to develop for large values of the parameter  $\lambda$ , such as increased CP-even Higgs masses (making low values of  $\tan\beta \sim 1 - 2$  acceptable) or reduced charged Higgs masses.

EWPOs were already partially discussed in the NMSSM: [20] dedicates particular interest to the  $Z \rightarrow b\bar{b}$  channel, where the experimental result shows a discrepancy of about  $\sim 3\sigma$  with the SM prediction, with the conclusion that this feature could not be improved in the NMSSM. [21] studied  $Z$ -decays involving very-light CP-odd Higgs bosons, *e.g.* in the NMSSM, in view of future searches at GigaZ. Yet, the details of the NMSSM phenomenology in view of the EWPOs, and especially in its specific scenarii, has been little discussed so far. This paper focuses therefore, in the context of the NMSSM, on the relation of the  $W$  mass  $M_W$  to the other parameters of the gauge sector: the  $Z$ -mass  $M_Z$ , the Fermi constant  $G_\mu$  (obtained from muon decays) and the fine-structure constant  $\alpha$ . Leptonic  $Z$ -decays in the NMSSM are also discussed. We find that most of the NMSSM, in its allowed parameter space (in view of stability conditions, phenomenological constraints from LEP,  $B$ - or  $\Upsilon$ -physics, . . .), is consistent with existing bounds on  $M_W$  and leptonic  $Z$ -decays. The leading new-physics effects are associated with the supersymmetric sector (provided the SUSY spectrum is rather light), hence MSSM-like. NMSSM-specific effects associated with the Higgs sector are essentially determined by the mass of the light doublet state and Standard-Model-like. In the following section, we detail our calculation of  $M_W$  and leptonic  $Z$ -decays in the context of the NMSSM. In the third section, we will discuss our results for the NMSSM, with particular emphasis on NMSSM-specific scenarii. In the remaining part of the introduction, we shall summarize the current experimental and SM status of those observables that we plan to discuss.

The current experimental value of  $M_W^{\text{exp.}} = 80.399 \pm 0.023$  GeV originates from a combined fit of LEP and TeVatron measurements [2, 3]. Future improvements should reduce the error down to 15 MeV [4] and 7 MeV [5] at LHC and GigaZ respectively. In the SM, one-loop [22] and two-loop [23, 24] corrections as well as leading higher order effects (to the parameter  $\Delta\rho$ ) [25] have been computed, leading to an estimated theoretical error of about 4 MeV [24]. Several computer codes (TOPAZO [26], ZFitter [27, 28], GFitter [29]) evaluate this quantity, relying on fitting expressions such as eq. 5.2-5.4 in [28]. The uncertainties on the top mass  $m_t = 172 \pm 1.6$  GeV,  $M_Z = 91.1876 \pm 0.0021$  GeV,  $\alpha_S(M_Z) = 0.1184 \pm 0.0004$  and the fermionic shift of the fine structure constant  $\Delta\alpha = 0.05907 \pm 0.0004$  [30] yield an additional parametric error, which we evaluate by varying these quantities within eq. 5.2-5.4 of [28]. Assuming (arbitrarily) a SM Higgs mass of  $M_H^{SM} = 150$  GeV (as we will all along this paper, except in plots, when otherwise mentioned), we eventually come to a SM estimate:  $M_W^{SM}(M_H^{SM} = 150 \text{ GeV}) = 80.343 \pm (0.012)^{\text{param.}} \pm (0.004)^{\text{high. ord.}}$  GeV, where the parametric errors, being mainly from experimental origins, were summed quadratically. The slight tension with the experimental value may of course be mended by a smaller choice of  $M_H^{SM}$ , although, for  $M_H^{SM} \geq 114$  GeV, the central value always remains smaller than the experimental one.

We will also consider leptonic decay modes of the  $Z$  boson, in particular, possible deviations from universality between the channels  $Z \rightarrow e^+e^-$  and  $Z \rightarrow \tau^+\tau^-$  (which, to our knowledge, has been little exploited so far, even in the MSSM). The total width of the  $Z$  boson is given experimentally by  $\Gamma_Z^{\text{exp.}} = (2.4952 \pm 0.0023)$  GeV. The leptonic decay modes  $Z \rightarrow l^+l^-$  are characterized by the experimental branching ratios [2, 30]:  $BR(Z \rightarrow e^+e^-)^{\text{exp.}} = (3.363 \pm 0.004) \cdot 10^{-2}$  and  $BR(Z \rightarrow \tau^+\tau^-)^{\text{exp.}} = (3.367 \pm 0.008) \cdot 10^{-2}$ . Moreover, the relative importance of these modes is determined by  $(\Gamma(Z \rightarrow \tau^+\tau^-)/\Gamma(Z \rightarrow e^+e^-) - 1)^{\text{exp.}} = (1.9 \pm 3.2) \cdot 10^{-3}$ .

On the theoretical side, the leptonic decay modes are described by the following expression of the decay width into a pair of leptons ( $l^+l^-$ ; see *e.g.* [8]):

$$\Gamma(Z \rightarrow l^+l^-)^{\text{theo.}} = \frac{G_\mu(1 - \Delta r)}{6\sqrt{2}\pi} M_Z^3 \left\{ (g_V^{l,\text{eff}})^2 \left[ \sqrt{1 - \frac{4m_l^2}{M_Z^2}} \left( 1 + \frac{2m_l^2}{M_Z^2} \right) + \frac{3}{4\pi} \bar{\alpha}(M_Z) \right] + (g_A^{l,\text{eff}})^2 \left[ \sqrt{1 - \frac{4m_l^2}{M_Z^2}} \left( 1 - \frac{4m_l^2}{M_Z^2} \right) + \frac{3}{4\pi} \bar{\alpha}(M_Z) \right] \right\} \quad (1)$$

$G_\mu = (1.16637 \pm 0.00001) \cdot 10^{-5}$  is the Fermi constant measured in muon decays.  $\bar{\alpha}(M_Z) \simeq 1/127.92$  is the

running fine-structure constant at the  $Z$ -pole.  $\Delta r$  corresponds to the (non-QED) loop corrections to this measurement (related to  $M_W$ : see eq. 5 below).  $g_V^{l,\text{eff}}$  and  $g_A^{l,\text{eff}}$  parametrize the  $Zl^+l^-$  effective vertex:

$$\Gamma_{Zll}^\mu = \left(\sqrt{2}G_\mu(1 - \Delta r)\right)^{1/2} M_Z \gamma^\mu \left[g_V^{l,\text{eff}} - \gamma_5 g_A^{l,\text{eff}}\right] \quad (2)$$

$$= (\sqrt{2}G_\mu \rho_l)^{1/2} M_Z \gamma^\mu \left[-2Q_l \sin^2 \theta_{\text{eff}}^l + I_3^l(1 - \gamma_5)\right] \quad (3)$$

where we introduce the second parameterization (see *e.g.* [1]) in terms of the form factor  $\rho_l$  and the effective leptonic weak mixing angle  $\theta_{\text{eff}}^l$  ( $Q_l = -1$  and  $I_3^l = -1/2$  are respectively the charge, in units of  $e$ , and the weak isospin of the lepton  $l$ ). At tree level,  $g_V^{l,\text{tree}} = I_3^l - 2Q_l s_W^2$  and  $g_A^{l,\text{tree}} = I_3^l$ .

In the SM, the form factor  $\rho_l^{SM} \simeq 1.005165$  [28] is known with a theoretical uncertainty of about  $2 \cdot 10^{-5}$  (with respect to higher orders). All uncertainties considered, we will assume an error of  $2 \cdot 10^{-4}$  on this quantity.  $\sin^2 \theta_{\text{eff}}^{l,SM}$ , similarly to  $M_W$ , has been computed beyond two-loop accuracy [31] and can be evaluated through numerical approximate formulae (see *e.g.* eq. 5.7-5.9 in [28]), with an estimated theoretical error of  $4.9 \cdot 10^{-5}$ . Using eq. 5.7-5.9 of [28] (with a Higgs mass  $M_H^{SM} = 150$  GeV), we obtain  $\sin^2 \theta_{\text{eff}}^{l,SM} = 0.23164 \pm (0.00015)^{\text{param.}} \pm (0.00005)^{\text{high. ord.}}$ . At the level of the branching ratios, we get:  $BR(Z \rightarrow e^+e^-)^{SM} \simeq 3.365 \cdot 10^{-2}(1 \pm 1 \cdot 10^{-3})$  and  $BR(Z \rightarrow \tau^+\tau^-)^{SM} \simeq 3.358 \cdot 10^{-2}(1 \pm 1 \cdot 10^{-3})$ , where all the errors have been added in quadrature.

Alternatively to the branching ratios, one may consider directly the effective leptonic Weinberg angle:

$$\sin^2 \theta_{\text{eff}}^l = \frac{1}{4|Q_l|} \left(1 - \frac{g_V^{l,\text{eff}}}{g_A^{l,\text{eff}}}\right) \quad (4)$$

This quantity is extracted from experimental measurements:  $(\sin^2 \theta_{\text{eff}}^l)^{\text{exp.}} = 0.23153 \pm 0.00016$  [2]. The corresponding SM prediction is quoted in the paragraph above eq. 4.

## 2 New Physics contributions to the EWPOs in the NMSSM

In this section, we shall detail the new contributions, beyond the SM, to  $M_W$  and the leptonic  $Z$ -decays in the NMSSM that we take into account and discuss how these are incorporated in our implementation of the observables.

### 2.1 $M_W$ in the NMSSM

The very precise measurement of the Fermi constant  $G_\mu$  is extracted from the muon decay  $\mu \rightarrow e\nu_\mu\bar{\nu}_e$ . In the SM and its extensions, such a decay can also be computed in terms of gauge couplings, which allows to relate  $G_\mu$  to other electroweak quantities (see *e.g.* [9] for a more detailed discussion):

$$\frac{G_\mu}{\sqrt{2}} = \frac{\pi\alpha}{M_W^2 \left(1 - \frac{M_W^2}{M_Z^2}\right)} (1 + \Delta r(M_W, M_Z, \dots)) \quad (5)$$

where  $\alpha \simeq 1/137.03599911$  is the fine-structure constant.  $\Delta r$  encompasses the (non-QED) loop corrections and is model-dependent. Eq. 5 can be inverted, leading to an (implicit, since  $\Delta r$  depends itself on  $M_W$ ) expression of the  $W$  mass in terms of  $M_Z$ ,  $G_\mu$ , etc.:

$$M_W^2 = \frac{M_Z^2}{2} \left[1 + \sqrt{1 - \frac{4\pi\alpha}{\sqrt{2}G_\mu M_Z^2} (1 + \Delta r(M_W, M_Z, \dots))}\right] \quad (6)$$

Starting from a reference value  $M_W^{2(0)}$ , for which we choose  $M_W^{2(0)} = M_W^{2,SM}(M_H^{SM} = 150 \text{ GeV})$ , the contribution to eq. 6 at leading-order in  $\delta M_W^2 = M_W^2 - M_W^{2(0)}$  (*i.e.* in  $\Delta r$ ) can be obtained directly by evaluating  $\Delta r(M_W^{2(0)})$ . Only at higher order need we take the shift of the right-hand-side of eq. 6, induced by  $\delta M_W^2$ , into account. The traditional approach consists then in iterating eq. 6 a few times. An alternative method

consists in Taylor-expanding the right-hand-side of eq. 6 at  $M_W^2 = M_W^{2(0)} + \delta M_W^2$ : for a calculation of eq. 6 at second order in  $\delta M_W$ ,  $\Delta r$  needs to be expanded at first order, leading to terms  $\propto \Delta r(M_W^{2(0)})$ , which should consistently be evaluated at second order, and terms  $\propto d\Delta r/dM_W^2(M_W^{2(0)})$ , which need only be evaluated at leading order. We compared both methods, which, given the uncertainty, led to similar results.

Given the far-superior (beyond two-loop) accuracy of the SM calculation, we split  $\Delta r^{NMSSM} = \Delta r^{SM} + \Delta r^{NP}$ , where  $\Delta r^{NP}$  contains all the new-physics contributions (and subtracts the absent SM contributions, in particular from the SM Higgs). At leading (one-loop) order,

$$\Delta r^{NP,1l.} = \left[ \frac{\hat{\Sigma}_W(0)}{M_W^2} + 2\delta^v + \delta^b \right]_{NMSSM-SM} \quad (7)$$

where  $\hat{\Sigma}_W(0)$  is the (transverse)  $W$  renormalized self-energy at 0 momentum while  $\delta^v$  and  $\delta^b$  summarize vertex and box corrections to the decay  $\mu \rightarrow e\nu_\mu\bar{\nu}_e$  (here, we will neglect the light lepton masses and assume universality in the slepton spectrum for the first two generations).  $\Delta r^{NP,1l.}$  may be further separated into contributions from the modified Higgs sector (the corresponding contributions to  $\delta^v$  and  $\delta^b$  vanish in the approximation  $m_e = 0 = m_\mu$ ) and contributions from the supersymmetric particles, sleptons, charginos and neutralinos. We computed these one-loop contributions anew and found agreement with the existing literature (see *e.g.* [20]). The corresponding calculation is formally identical to that in the MSSM [32], were it not for the presence of two additional Higgs and one additional neutralino states in the NMSSM. Note that in the MSSM, non-minimal flavour-violating [33] and CP-violating [9, 34] effects were also investigated.

Higher order corrections should be included through an expansion of the resummation formula [35]:  $1 + \Delta r = \left( (1 + \Delta\alpha)(1 + \frac{c_W^2}{s_W^2}\Delta\rho) - \Delta r_{rem.} \right)^{-1}$ . Corrections of order  $\alpha\alpha_S$  to the parameter  $\Delta\rho$  were computed for the MSSM [36]: beyond the SM-like effects, they arise from gluon/squark and gluino/squark diagrams. Such contributions are identical in the NMSSM and the MSSM, hence may be included in the calculation directly. However, we will always consider heavy gluinos so that the gluino effects remain negligible. Additional  $O(Y_i Y_j / (4\pi)^2)$  contributions,  $Y_{i,j} = Y_t, Y_b$  being the top and bottom Yukawa couplings, were calculated in the MSSM [37], including SM-like quark/Higgs as well as supersymmetric higgsino/squark diagrams. Such effects cannot be incorporated so straightforwardly in the NMSSM. However, we note that most of such effects are captured by the corresponding SM contribution, contained in  $\Delta r^{SM}$ , that we will not subtract.

To compute the error estimate, we considered the analysis in [10] for the MSSM as well as the magnitude, for the MSSM, of those higher-order contributions which are known in the MSSM but neglected in our computation. We therefore decided to include a higher-order uncertainty of about 10 MeV (when squarks are all heavier than  $\sim 500$  GeV) to 20 MeV (for squark masses below  $\sim 500$  GeV) for  $M_W$ . To define our “exclusion” limits, we double the SM parametric error and add linearly the SM and SUSY higher-order uncertainties.

## 2.2 New Physics contributions to $g_{V,A}^{l,eff}$

We already introduced the general formalism associated with  $Z \rightarrow l^+l^-$  decays (eq. 1, 2). Again, we split  $g_{V,A}^{l,eff} = (g_{V,A}^{l,eff})^{SM} + (g_{V,A}^{l,eff})^{NP}$ . Note however that a “hidden contribution” already intervenes at tree-level in  $g_{V,A}^{l,eff}$ : as we analysed in the previous subsection, radiative corrections induce a shift in the determination of  $M_W$ , which, in turn, results in a shift of the Weinberg angle.

The new physics contributions to  $g_{V,A}^{l,eff}$  were computed (at the  $Z$ -pole) at the one-loop level according to (see *e.g.* [20]):

$$\begin{cases} (g_V^{l,eff})^{NP} = \left[ \Gamma_V(M_Z^2) - g_V^{l,trec} \Sigma_V^l(m_l^2) - g_A^{l,trec} \Sigma_A^l(m_l^2) - g_A^{l,trec} \frac{c_W}{s_W} \frac{\Sigma^{\gamma Z}(0)}{M_Z^2} - \frac{1}{2} g_V^{l,trec} \hat{\Sigma}'_Z(M_Z^2) \right. \\ \left. - 2 \frac{c_W s_W}{M_Z^2} \hat{\Sigma}^{\gamma Z}(M_Z^2) \right]_{NMSSM-SM} \\ (g_A^{l,eff})^{NP} = \left[ \Gamma_A(M_Z^2) - g_V^{l,trec} \Sigma_A^l(m_l^2) - g_A^{l,trec} \Sigma_V^l(m_l^2) - g_A^{l,trec} \frac{c_W}{s_W} \frac{\Sigma^{\gamma Z}(0)}{M_Z^2} - \frac{1}{2} g_V^{l,trec} \hat{\Sigma}'_Z(M_Z^2) \right]_{NMSSM-SM} \end{cases} \quad (8)$$

where  $\Gamma_{V,A}(M_Z^2)$  denote the  $Zll$  (1PI) vertex corrections at the  $Z$ -pole,  $\Sigma_{V,A}^l$  stand for the lepton ( $l$ ) self-energies,  $\Sigma_Z$  and  $\Sigma^{\gamma Z}$ , for the  $Z$  and  $\gamma Z$  self-energies. The hat  $\hat{\phantom{x}}$  signals renormalized self-energies and the prime  $'$ , derivatives with respect to the external 4-momentum squared. The indices  $V$  and  $A$  still denote vector and axial(-vector) contributions.

Again, the new contributions arise from the NMSSM Higgs sector (from which the 1-loop contribution of the SM Higgs is subtracted) as well as supersymmetric particles (*e.g.* Higgs/lepton and chargino or neutralino/sleptons diagrams in  $\Gamma_{V,A}$ ). Our calculation agrees with the existing literature (see *e.g.* [20]). However, we also incorporate higher-order corrections in the form of corrected Yukawa couplings, relevant for large  $\tan\beta$  (see *e.g.* [38]):

$$Y_l = \frac{m_l \tan\beta}{v(1 + \varepsilon_l \tan\beta)} \quad (9)$$

We allow for a 30% uncertainty on the gauge contributions to  $(g_{V,A}^{l,\text{eff}})^{NP}$ , where QCD corrections may intervene at the two-loop level. However, we confine ourselves to a 10% error on the leptonic part ( $\Gamma_{V,A}$  and  $\Sigma_{V,A}^l$ ) where no strong coupling should arise at the following order. Error estimates on  $(g_{V,A}^{l,\text{eff}})^{SM}$  are extracted from the uncertainty on  $\rho_l^{SM}$  and  $\sin^2\theta_{\text{eff}}^{l,SM}$ , which was presented in the introduction. These SM and NP uncertainties are added linearly. At the level of the branching ratios, they are then combined quadratically with the ( $2\sigma$ ) error on the experimental input ( $M_Z, G_\mu, \Gamma_Z$ ) to define the error estimate.

The observable  $(\Gamma(Z \rightarrow \tau^+\tau^-)/\Gamma(Z \rightarrow e^+e^-) - 1)$  should be sensitive to possible deviations from universality. Using eq. 1 (at first order in  $m_\tau^2/M_Z^2$  and neglecting  $m_e^2 \ll m_\tau^2, M_Z^2$ ), we derive:

$$\frac{\Gamma(Z \rightarrow \tau^+\tau^-)}{\Gamma(Z \rightarrow e^+e^-)} - 1 = \frac{[(g_{V,A}^{\tau,\text{eff}})^2 - (g_{V,A}^{e,\text{eff}})^2 + (g_A^{\tau,\text{eff}})^2 - (g_A^{e,\text{eff}})^2] - \frac{6m_\tau^2(g_A^{\tau,\text{eff}})^2}{M_Z^2(1 + \frac{3}{4\pi}\bar{\alpha}(M_Z))}}{(g_{V,A}^{e,\text{eff}})^2 + (g_A^{e,\text{eff}})^2} \quad (10)$$

To estimate the error on  $(g_{V,A}^{\tau,\text{eff}})^2 - (g_{V,A}^{e,\text{eff}})^2 \simeq 2g_{V,A}^{e,\text{eff}}(g_{V,A}^{\tau,\text{eff}} - g_{V,A}^{e,\text{eff}})$ , we retain 10% of the universality-deviating contributions (Higgs and supersymmetric sectors, with no QCD corrections at two-loop) in  $g_{V,A}^{\tau,\text{eff}} - g_{V,A}^{e,\text{eff}}$ , to which we add a fixed error amounting to  $10^{-3} \cdot g_{V,A}^{e,\text{eff}}$  for neglected orders of a different type.

### 3 Numerical results

The observables are included in a fortran code as prescribed in the previous section. This program is then coupled to the NMSSMTools 2.3.2 package [39], computing the NMSSM spectrum and checking already several phenomenological constraints: stability of the electroweak vacuum, bounds from LEP [12], and in particular the new ALEPH limits [17]<sup>1</sup>, from  $B$ - and  $\Upsilon$ -physics [40,41], etc. Note that the NMSSM contribution to the anomalous magnetic moment of the muon is also computed [42]. However, given the still unclear situation concerning the agreement of  $\tau$ - and  $e^+e^-$ -based SM hadronic contributions to this observable, we will regard a SM-like result as allowed (although  $\gtrsim 3\sigma$  away from the experimental measurement, when using  $e^+e^-$ -data; see *e.g.* [43] for a recent analysis). First, we will discuss  $M_W$  and the leptonic  $Z$ -decays in the MSSM limit of the NMSSM. Then, we will turn to specific NMSSM effects.

#### 3.1 MSSM limit

The MSSM limit of the NMSSM is obtained by choosing small parameters  $\lambda \sim \kappa \ll 1$  while keeping  $\mu_{eff} \propto \lambda/\kappa$  at the electroweak-TeV scale. In this case, the NMSSM would be undistinguishable, in collider phenomenology, from a genuine MSSM, except for possible dark matters effects (in case of a singlino LSP). Note that most NMSSM effects in the EWPOs (*e.g.* from supersymmetric particles) may be expected to be MSSM-like and this subsection is meant to summarize such results as well as serve for comparison with specific NMSSM effects, which will be discussed separately.

<sup>1</sup>A bug in the corresponding version of the code for the computation of ALEPH constraints was replaced by a self-made program. This problem was fixed, in the meanwhile, in the version 2.3.3 of NMSSMTools.

The impact of a MSSM-like Higgs sector is illustrated by Fig. 1:  $M_W$  and  $\sin^2 \theta_{\text{eff}}^\tau$  are plotted against the charged-Higgs mass  $m_{H^\pm}$  (controlling the mass of the heavy MSSM-like approximate  $SU(2)_L$  doublet). The supersymmetric spectrum was chosen very heavy with sfermion, chargino and neutralino masses of about  $\sim 2$  TeV, so as to suppress associated effects. Consequently the effects are found to be very small as long as  $m_{H^\pm} \gtrsim 250$  GeV, with *e.g.*  $M_W$  almost entirely determined by the SM-result applied to its lightest doublet mass ( $\sim 117$  GeV in the considered case). Low values of  $m_{H^\pm}$  (as the whole Higgs spectrum becomes light) would tend to increase  $M_W$  (hence improving its agreement with the experimental value), decrease  $\sin^2 \theta_{\text{eff}}^\tau$  (hence worsening its agreement with experiment), but such effects become significant mainly for mass ranges already excluded by LEP constraints. We therefore conclude that the impact of the MSSM Higgs sector is mainly driven by the lightest CP-even (doublet) Higgs, whose mass is almost as strongly bound by LEP-constraints as that of its SM alter ego. In contrast, unconventional scenarii are possible in the NMSSM CP-even Higgs spectrum, and this is where specific NMSSM effects are expected.

We then consider effects associated with the supersymmetric spectrum (and settle for a heavy Higgs doublet mass of  $\sim 500$  GeV): such contributions are essentially common to the MSSM and the NMSSM, since the NMSSM spectrum, except for an additional (but usually almost decoupled) neutralino state (the singlino), is similar to that of the MSSM. In Fig. 2, the sfermion sector is kept very heavy  $\sim 2$  TeV and we vary the mass of the supersymmetric fermions (gauginos/higgsinos) according to the hierarchy  $2M_1 = M_2 = \mu_{\text{eff}} = M_3/3 \equiv m_\chi$ . We find that a light gauginos-higgsino sector can increase  $M_W$  of a few 10 MeV, while its effect on the other observables remains small (note that this will not remain the case for lighter sfermion spectra). In Fig. 3, we scan over a common soft SUSY-breaking sfermion mass  $m_{\text{sf.}}$ . Note, however, that the left-right sfermion mixing may remain large (trilinear soft couplings are kept at  $-1$  TeV, while  $\mu_{\text{eff}} = 400$  GeV), so that even for small  $m_{\text{sf.}}$ , one of the stops (and sbottoms) is sensibly heavy, sufficiently to generate a CP-even Higgs mass beyond LEP bounds. Lighter sfermion spectra contribute to the predicted  $M_W$ , and may improve its agreement with the experimental measurement, but they correspondingly increase the tension in  $\sin^2 \theta_{\text{eff}}^\tau$ , which (expectedly) shows a behaviour “opposite” to  $M_W$ . Note that, as  $M_W$  increases, the  $SU(2)_L$  interaction strengthens, leading to a larger  $BR(Z \rightarrow \tau^+ \tau^-)$  (which is not shown but essentially remains within the  $1\sigma$  experimental range). No deviation from lepton universality is observed: note that slepton states are still heavy while the lightest stop mass approaches the electroweak scale (due to the more efficient stop mixing). We stress that these supersymmetric effects generically prove the most significant contributions in both the MSSM and the NMSSM, and explain how supersymmetric extensions of the SM, albeit often subject to comparable limits on the mass of the lightest CP-even Higgs as the SM, can improve the agreement of the theoretical predictions for EWPOs (and more specifically  $M_W$ ) with the corresponding experimental values.

Now, we wish to consider flavour effects and, since we consider leptonic observables, we vary the common soft SUSY-breaking stau mass  $m_{\tilde{\tau}}$  and show the impact on  $M_W$  and  $\Gamma(Z \rightarrow \tau^+ \tau^-)/\Gamma(Z \rightarrow e^+ e^-) - 1$  in Fig. 4. Several choices of the trilinear  $A_\tau$  coupling and  $\mu_{\text{eff}}$ , regulating the mixing of staus ( $\propto m_\tau (A_\tau - \mu_{\text{eff}} \tan \beta)$ ), are studied. We choose a large value for  $\tan \beta = 40$ , enhancing leptonic Yukawa couplings. Deviations of  $M_W$  occur for small stau masses and can reach up to  $\sim 10$  MeV in the allowed slepton mass range. We observe that this effect can be suppressed, even reversed, when mixing among the staus becomes efficient. We also notice that a light slepton ( $\sim 300$  GeV) sector is sufficient to bring the theoretical prediction of  $M_W$  within its experimental  $1\sigma$  error bars (at the expense of  $\sin^2 \theta_{\text{eff}}^\tau$  however, which is not shown but may lead to difficulties for very light sleptons  $\sim 150$  GeV). Deviations from lepton universality in  $Z$ -decays are generated for light slepton spectra and worsen the SM results with respect to the experimental limits. However, such effects remain essentially small and, given the current uncertainties, are not significant.

Finally, Fig. 5 shows the variations of  $M_W$  and  $\Gamma(Z \rightarrow \tau^+ \tau^-)/\Gamma(Z \rightarrow e^+ e^-) - 1$  in terms of  $\tan \beta$  for heavier/lighter slepton and gaugino-higgsino sectors. The significant effects (in  $M_W$ ) observed at low  $\tan \beta$  correspond to light CP-even Higgs masses, already excluded by LEP. Light supersymmetric spectra tend to shift  $M_W$  upwards as we already discussed. Small flavour effects appear at large  $\tan \beta$  (in  $\Gamma(Z \rightarrow \tau^+ \tau^-)/\Gamma(Z \rightarrow e^+ e^-) - 1$ ) for light sleptons, but remain negligible in comparison to the uncertainty, all the more that large  $\tan \beta$  regions are already constrained by  $B$ -physics observables (such as  $BR(\bar{B}_s^0 \rightarrow \mu^+ \mu^-)$ ).

As a summary for this analysis of the MSSM limit (hence of MSSM-like NMSSM effects), most of the MSSM, within its allowed parameter space (in view of bounds on direct searches of Higgs and supersymmetric particles,  $B$ -physics), lies within the allowed range of the considered observables, and only weak

constraints can thus be extracted, except perhaps for very light sfermion spectra (in view of  $\sin^2 \theta_{\text{eff}}^\tau$ ). Future experimental developments may lead to more significant limits, although a comparable accuracy from the theoretical side might prove difficult to achieve (note, however, that a large portion of the theoretical error is parametric and will therefore be reduced along with the experimental uncertainty on  $m_t$ , etc.). New physics effects lie essentially in light supersymmetric spectra ( $\sim 100 - 300$  GeV) and may improve the agreement of the theoretically predicted  $M_W$  with its experimental determination. Note however that tensions might then correspondingly arise in  $\sin^2 \theta_{\text{eff}}^\tau$ . Higgs effects are mainly controlled by the mass of the SM-like CP-even Higgs. Finally, effects violating lepton universality tend to increase the tension with experimental measurements, but remain small (below the uncertainty) in the available parameter space: universal contributions are found to dominate.

### 3.2 NMSSM at low $\tan \beta$

We will now consider specific NMSSM effects, hence use  $\lambda$  (or  $\kappa$ ) of order 1 (Note that, in order to ensure the perturbativity of such couplings up to a Grand-Unification scale, one must require  $\lambda \lesssim 0.8$ : see *e.g.* Fig. 1 of [13]). These new effects are essentially expected in the Higgs sector since, except for the additional singlino state, the rest of the spectrum is essentially MSSM-like. Note however, that a first consequence of the modified Higgs sector consists in an enlarged parameter space, allowing for low values of  $\tan \beta \sim 1 - 2$ , despite LEP constraints: large  $\lambda$  generates indeed an additional contribution to the light CP-even doublet Higgs mass at tree-level, so that the maximal mass is actually reached at low  $\tan \beta$ , provided  $\lambda v \gtrsim M_Z$ . In contrast, the MSSM cannot generate sufficiently large Higgs masses in this regime, leading to the exclusion of low  $\tan \beta$ .

As explained above, we focus on Higgs effects, which, in the MSSM limit, were found dominated by the SM-like contribution of the light doublet state. The same remains true for the low  $\tan \beta$  NMSSM, as can be observed in Fig. 6 (with a heavy SUSY scale  $\sim 2$  TeV):  $M_W$  and  $\sin^2 \theta_{\text{eff}}^\tau$  are shown in terms of the lightest CP-even Higgs mass (in this case almost purely doublet) and found almost identical to the SM-predictions for similar Higgs masses. Note that the low  $\tan \beta$  effect on Fig. 5, in the excluded range of the MSSM limit, was simply associated with the MSSM light CP-even state becoming light (hence violating LEP constraints): this behaviour characterizes in no way that of the low- $\tan \beta$  NMSSM where the light CP-even Higgs mass need also exceed  $\sim 114$  GeV to escape LEP bounds (except in specific scenarii which will be discussed in the following subsections). Naturally, lighter SUSY spectra can be associated to this regime, leading to increased  $M_W$  as we discussed for the MSSM limit.

### 3.3 NMSSM Light CP-odd Higgs

In the NMSSM, light CP-odd Higgs states  $A_1$  (as light as a few GeV) represent an interesting phenomenological possibility. Such particles have indeed vanishing  $V - V - A_1$  ( $V = W, Z$ ) couplings which allows them to circumvent most of the direct collider constraints.  $B$ -physics processes [40], in particular  $\bar{B}_s^0 \rightarrow \mu^+ \mu^-$  or  $\bar{B}_s^0 \rightarrow X_s \mu^+ \mu^-$ , and  $\Upsilon$  decays [41], for  $m_{A_1} \leq m_\Upsilon$ , constrain however significantly large values of the reduced-coupling of the  $A_1$  to down-type quarks,  $X_d \equiv \cos \theta_A \tan \beta$ , where  $\cos \theta_A$  quantifies the amount of doublet component in the  $A_1$ . The very-light mass ( $m_{A_1} \lesssim 5$  GeV) region was shown to be already essentially excluded [44]. The light NMSSM CP-odd Higgs is often associated with the so-called ‘‘Ideal Higgs scenario’’, which we will discuss in the next subsection and in which case it must satisfy  $m_{A_1} < 2 m_B$  to forbid kinematically the *a priori* dominant  $A_1 \rightarrow b\bar{b}$  decay channel and circumvent bounds from CP-even Higgs searches at LEP. Yet, in general, light  $A_1$  are not necessarily associated with specifically light CP-even Higgs ( $h_1$  could be as heavy as  $\sim 140$  GeV in the NMSSM), hence offer a wider phenomenological possibility than the ‘‘Ideal Higgs scenario’’. In two limits of the parameter space (R symmetry, with vanishing Higgs trilinear soft couplings; Peccei-Quinn symmetry, with  $\frac{\kappa}{\lambda} \ll 1$ ), the  $A_1$  is the Nambu-Goldstone boson of an approximate and spontaneously-broken global symmetry, which justifies the naturality of its lightness. Note that in such cases,  $X_d$  remains in general small and the decoupled  $A_1$  proves hard to probe experimentally.

We investigate the effects of a light CP-odd Higgs on  $BR(Z \rightarrow \tau^+ \tau^-)$  and  $\Gamma(Z \rightarrow \tau^+ \tau^-)/\Gamma(Z \rightarrow e^+ e^-) - 1$  in Fig. 7 (the effects on  $M_W$  and  $\sin^2 \theta_{\text{eff}}^\tau$  were found negligible). Expectedly, a light CP-odd Higgs can contribute to these observables when its reduced-coupling to leptons (and down-type quarks)  $X_d$

is enhanced. The corresponding contribution is found to worsen the agreement of the theoretical prediction with the experimental limits. Yet, even fairly large values of  $X_d$  (such as  $\sim 25$  in Fig. 7) remain compatible with the current precision. In view of the upper-bounds placed on  $X_d$  by  $B$ - and  $\Upsilon$ -processes [40, 41] ( $X_d \lesssim 2 - 3$ , for  $m_{A_1} \lesssim 10$  GeV), we may conclude that the light- $A_1$  scenario is consistent with leptonic  $Z$ -decays.

### 3.4 Light CP-even doublet-like Higgs

A widely-studied NMSSM-specific scenario is that of a CP-even (doublet) Higgs decaying unconventionally into a pair of light CP-odd Higgs (below the  $B - \bar{B}$  threshold), hence escaping LEP constraints from  $e^+e^- \rightarrow Z(h_1 \rightarrow b\bar{b})$ , so that  $m_{h_1} \sim 90 - 100$  GeV remains phenomenologically viable. It was even argued that  $m_{h_1} \sim 98$  GeV could be used as an interpretation of the  $2.3\sigma$  excess found in  $e^+e^- \rightarrow Z(h_1 \rightarrow b\bar{b})$ , leading to an ‘‘Ideal Higgs scenario’’ [19]. The recent ALEPH analysis on  $e^+e^- \rightarrow Z(h_1 \rightarrow 2A_1 \rightarrow 4\tau)$  [17] seems, however, to constrain efficiently such a scenario, although possible ways out, such as reduced  $BR(A_1 \rightarrow \tau^+\tau^-)$  decays for  $\tan\beta \sim 1 - 2$  [18], have been suggested.

In the following, we will consider a specific realization of this light doublet-Higgs scenario where ALEPH bounds may also be circumvented. An approximate Peccei-Quinn symmetry (characterized by  $\kappa/\lambda \sim O(10^{-1}) \ll 1$ ) protects the light CP-odd Higgs mass (although the R symmetry is more frequently used), hence allowing for the unconventional channel  $h_1 \rightarrow 2A_1$  (with  $m_{A_1} < 2m_B$ ), while  $\lambda \sim 0.5$  is relatively large (hence allowing for specific NMSSM effects). In this setup, the CP-odd Higgs is essentially singlet and its effect on  $M_W$  can be neglected. The two CP-even light states are essentially the doublet MSSM-like state and the singlet component. Due to the large  $\lambda$ , they can mix efficiently (while the heavy doublet decouples). Therefore, the lightest CP-even state, albeit dominantly doublet, carries a non-(necessarily) negligible singlet component. This leads, in turn, to a reduced production cross-section. We found realizations of this scenario for  $\tan\beta$  in the range  $2 - 12$ . Three factors ‘‘conspire’’ to circumvent LEP and in particular the ALEPH limits in this case:

- The unconventional  $h_1$  decay  $h_1 \rightarrow 2A_1$  is the dominant channel and explains the invisibility of  $h_1$  in the  $b\bar{b}$  channel at LEP. Note however that  $BR(h_1 \rightarrow 2A_1)$  need not be exactly 1 ( $\sim 0.8$  still guarantees the invisibility of  $h_1$  in  $b\bar{b}$  decays, for  $m_{h_1} \sim 95 - 100$  GeV).
- The production cross-section  $e^+e^- \rightarrow Zh_1$  is slightly reduced (with respect to the SM cross-section), due to the small singlet component of  $h_1$  (by at least  $\sim 10\%$ ).
- $BR(A_1 \rightarrow \tau^+\tau^-) \sim 0.75 - 0.9 < 1$  (for  $m_{A_1} \sim 9 - 10$  GeV), due to secondary decay channels (in particular  $A_1 \rightarrow gg$ ).

We choose a significantly heavy sfermion sector  $m_{sf} = 1.2$  TeV  $= -A_{sf}$  and a hierarchical gaugino structure  $6M_1 = 3M_2 = M_3 = 1.2$  TeV. We checked numerically that the contribution of supersymmetric particles remained approximately constant in comparison to the Higgs effects. The light CP-odd Higgs mass is kept in the range  $9 - 10$  GeV. Being almost entirely singlet, it contributes negligibly to the considered observables.

The variations of  $M_W$  (and  $\sin^2\theta_{\text{eff}}^\tau$ ) as a function of the mass of the light CP-even state, in the range  $\sim [80, 120]$  GeV, are shown in Fig. 8, for fixed amounts of the subdominant singlet component  $S_{13}^2 \sim 0.15, 0.30, 0.45 (\pm 5 \cdot 10^{-3})$ . We observe that the effect, even though the light state is dominantly doublet, remains comparatively smaller than that of a SM Higgs in the corresponding mass range (were such masses still allowed for the SM). This observation may be easily understood. In our scan, the MSSM-like diagonal light Higgs mass (noted as  $m_{h^0}$ ; note that this quantity still benefits from a NMSSM mass contribution  $\propto \lambda v \sin 2\beta$ , as discussed in subsection 3.2) is kept approximately constant (since the SUSY masses do not vary). Consequently, for a fixed singlet component  $S_{13}^2$ , the lowering of  $m_{h_1}$  is associated to an increasing singlet-doublet mixing entry and a heavier second-lighter (singlet-like) state: the more efficient contribution of a lighter  $h_1$  to  $M_W$  is balanced by a decreased  $h_2$  contribution (with a  $\gtrsim 15\%$  doublet component). More quantitatively, whenever the propagators of the two light Higgs states intervene, *e.g.* in a gauge boson self-energy  $\Sigma_V$ , the efficient part of the Higgs couplings originates from their doublet ‘‘MSSM’’ component, that is  $g_{\text{NMSSM}}^{h_i} \propto \sqrt{1 - S_{i3}^2} g_{\text{MSSM}}^{h^0}$ . Therefore, with  $1 - S_{23}^2 \sim S_{13}^2$  (since the singlet is essentially distributed



among the two light states;  $q$  denotes the 4-momentum of the considered Higgs-line):

$$\Sigma_V^{\{h_1, h_2\}} \propto \left[ \frac{1 - S_{13}^2}{q^2 - m_{h_1}^2} + \frac{S_{13}^2}{q^2 - m_{h_2}^2} \right] (g_{\text{MSSM}}^{h^0})^2 \quad (11)$$

However, the diagonalization of the MSSM-like and singlet states gives  $m_{h^0}^2 \sim (1 - S_{13}^2)m_{h_1}^2 + S_{13}^2 m_{h_2}^2$ , so that  $(1 - S_{13}^2)[q^2 - m_{h_1}^2]^{-1} + S_{13}^2[q^2 - m_{h_2}^2]^{-1} \sim [q^2 - m_{h^0}^2]^{-1}$ , and we obtain that the Higgs contribution is approximately given by that of its MSSM-like diagonal component. The latter, however, is kept constant in our case, and cannot be significantly lowered anyway, since ALEPH constraints would exclude a pure doublet state for  $m_{h_1} \lesssim 103 - 105$  GeV (depending on the details of  $BR(A_1 \rightarrow \tau^+ \tau^-)$  and  $BR(h_1 \rightarrow A_1 A_1)$ ; note also that small  $\tan \beta \sim 1 - 2$  lead to reduced  $BR(A_1 \rightarrow \tau^+ \tau^-)$ , allowing for even lighter doublet-states [18]). Therefore, the NMSSM-Higgs effect we obtain is reduced and, in Fig. 8, the generated shift in  $M_W$  is only of a few MeV in the authorized  $m_{h_1}$  range (not violating ALEPH constraints).

Note however that we chose here a very specific realization of the unconventionally-decaying Higgs scenario, and that slightly larger effects might be generated by relaxing *e.g.* the Peccei-Quinn symmetry requirement. This is illustrated by Fig. 9, where we study a scatter plot obtained by varying all the parameters of the Higgs sector ( $A_\lambda$ ,  $A_\kappa$ ,  $\mu_{\text{eff}}$  and  $\kappa$ ) with the exception of  $\lambda = 0.5$  and  $\tan \beta = 5$ . Note that as we depart from the Peccei-Quinn limit, points with large  $S_{13}^2 > 15\%$  become scarce (because the diagonal singlet mass, no longer protected by small  $\kappa/\lambda$ , tends to be large and the CP-even singlet cannot couple as efficiently with the doublet). The pink points correspond to almost entirely doublet  $h_1$  states (so that  $m_{h_1} \sim m_{h^0}$ ) and we observe, expectedly, that they are scattered around the SM prediction for  $M_H^{SM} = m_{h_1}$  (which is, in the SM, excluded by LEP). Although slightly less efficient, points with larger  $S_{13}^2$  give comparable results.

Finally, we extend our analysis to the region  $\tan \beta = 1.5$ , with an approximate R-symmetry (which we implement by the requirement  $|A_{\lambda, \kappa}| < 50$  GeV) protecting the light CP-odd mass.  $\lambda = 0.5$  continues to ensure the possibility of specific NMSSM effects. The ALEPH limits are circumvented by the reduced  $BR(A_1 \rightarrow \tau^+ \tau^-)$  (at low  $\tan \beta$  [18]), although a small  $S_{13}^2$  ( $\lesssim 8\%$ ) also often intervenes. In the scatter plot of Fig. 10, we scan again over  $A_\lambda$ ,  $A_\kappa$ ,  $\mu_{\text{eff}}$  and  $\kappa$  (note that the allowed points we obtain all verify  $\kappa \sim 0.3 - 0.5$ ). The allowed points again cluster around the (excluded by LEP) SM central value for  $M_H^{SM} = m_{h_1}$ .

As a conclusion for this subsection, we find that the NMSSM scenario with light CP-even doublet-like Higgs in the mass-range [95 – 115] GeV allows for a specific contribution, similar to that a doublet SM or MSSM Higgs would have generated, were such low masses still phenomenologically allowed in these models. Note however that what mass seems determinant is the pure doublet (MSSM-like) mass  $m_{h^0}$  and not, in case of a mixing with the singlet, that of the light eigenstate  $m_{h_1}$ . Note again that in this analysis, we tried to isolate this specific Higgs effect by suppressing the contribution of supersymmetric particles ( $m_{\text{st.}} = 1.2$  TeV). In the general case however, SUSY effects also intervene and add to the Higgs effect.

### 3.5 Light CP-even singlet-like Higgs

In the following, we consider another popular Higgs scenario, where the lightest CP-even Higgs is singlet-like, hence circumvents LEP constraints in virtue of a reduced production cross-section in  $e^+ e^-$  collision. For a purely decoupled singlet, this particle can be in principle as light as a few  $\sim 10$  GeV but also has negligible effects on the doublet sector. We will thus rather focus on CP-even singlets with a sizable doublet component: we shall use  $S_{13}^2 \sim 80\%$  in Fig. 11, which satisfies LEP constraints provided  $m_{h_1} \gtrsim 40$  GeV. In this case, the singlet-doublet mixing uplifts the mass of the light doublet-like Higgs state  $h_2$ , with respect to the pure doublet mass  $m_{h^0}$  (due to the splitting effect).

We obtain a specific realization of this scenario in an approximate Peccei-Quinn limit of the parameter space  $\kappa/\lambda = 10^{-1} \ll 1$ ,  $\lambda \sim 0.5$ : the setup is comparable to that of subsection 3.4, but with an inverted hierarchy between the singlet and light-doublet states. Note that, neglecting the Peccei-Quinn violating terms, the tree-level diagonal squared mass of the singlet component is given by  $m_{S^0}^2 \simeq \frac{\lambda^2 v^2 A_\lambda \sin 2\beta}{2\mu_{\text{eff}}}$  and is naturally at the electroweak scale or smaller (since  $\sin 2\beta \ll 1$  for  $\tan \beta \gg 1$ ). Moreover, the singlet and light-doublet components can couple efficiently in the large  $\lambda$  regime so that significant mixing may be easily achieved.

In this setup, several remarkable effects may influence EWPOs:  $h_1$  is significantly lighter than LEP-bounds for doublet states and carries a sizable doublet component ( $\sim 20\%$  in Fig. 11); the mass of the “visible” light-doublet state receives a contribution from the singlet-doublet mixing, hence allows for reduced pure doublet masses  $m_{h_0}$ ; for the same reason, squark masses may be smaller, hence contribute more to  $M_W$ . This discussion is illustrated by Fig. 11, showing  $M_W$  and  $\sin^2 \theta_{\text{eff}}^\tau$  in terms of the mass of the observable Higgs state,  $m_{h_2}$ . Note that  $M_W$  now increases with  $m_{h_2}$ : as the  $h_2$  becomes heavy, the  $h_1$  state, carrying a 20% doublet component, becomes correspondingly light, due to the splitting effect between the light-doublet and singlet components, hence has an enhanced contribution to  $M_W$ . However, excessively light  $h_1$  ( $m_{h_1} \lesssim 40$  GeV for  $S_{13}^2 \sim 0.8$ ) are eventually constrained by LEP searches. Lighter sfermion spectra yield both an increased SUSY contribution and a reduced diagonal doublet mass. This last property implies that (for equivalent  $h_1$  masses)  $h_2$  is also lighter. The limiting factor for light sfermions in Fig. 11, however, was found to be the stability of the electroweak-symmetry breaking vacuum. As the agreement of  $M_W$  with its experimental measurement is improved, that of  $\sin^2 \theta_{\text{eff}}^\tau$  again worsens correspondingly, albeit still within acceptable proportions with respect to the error bars.

In Fig. 12, we show a scatter plot (over  $A_\lambda$ ,  $A_\kappa$  and  $\mu_{\text{eff}}$ ) for  $\lambda = 0.5$ ,  $\kappa/\lambda = 0.1$  and a dominantly singlet light CP-even Higgs state. We observe that Higgs effects may generate a large  $M_W$ , even though the observable Higgs is as heavy as  $\sim 140$  GeV. We stress that this effect is allowed in the NMSSM due essentially to the interplay between doublet and singlet CP-even states and is thence NMSSM-specific.

## 4 Conclusions

We have studied  $M_W$  and other electroweak observables associated with  $Z$  leptonic decays in the NMSSM. Similarly to the MSSM, most of the acceptable parameter space of this model is consistent with the present accuracy available for the corresponding observables. Such an agreement with respect to EWPOs shows the robustness of supersymmetry-inspired extensions of the SM with respect to the description of the electroweak-symmetry breaking.

As a general trend, new-physics (N/MSSM) effects are found to improve the theoretical prediction for  $M_W$  with respect to the SM (which however remains compatible with existing bounds), the leading new contribution originating from (moderately) light supersymmetric spectra ( $\sim 300 - 500$  GeV). Specific effects in the NMSSM are associated with its extended Higgs sector. Yet, most of the Higgs effects in the electroweak precision observables under consideration are related to the mass of the light CP-even doublet component, lying in the  $\sim [90, 140]$  GeV range in the NMSSM. Corresponding effects remain generally small with respect to the current precision, although fluctuations of  $M_W$  by a few MeV can be generated in scenarios with very light doublet-like states or efficient doublet-singlet mixings, as soon as a state with non-negligible (a few 10%) doublet component becomes light. In the presence of a heavy supersymmetric spectrum, the unconventional Higgs spectrum of the NMSSM could thus relieve the tension in  $M_W$ , even for an apparently-heavy observable Higgs boson.

The possible presence of a light CP-odd Higgs in the NMSSM spectrum may also affect the universality of leptonic  $Z$ -decays. Note that corresponding effects tend to worsen (albeit below significance) the agreement with the experimental values. Nevertheless, only large (unrealistic)  $A_1 \bar{l} l$  couplings would lead to a significant deviation, which, in view of existing bounds (and naturalness considerations), are unlikely. The possibility of light CP-odd states and, in particular, their involvement in specific NMSSM scenarios (through unconventional decays) thus remain essentially consistent with the observables under consideration.

Further information might be extracted from hadronic  $Z$ -decays, although existing studies [20] already showed that no improvement was to be expected in the  $Z \rightarrow b\bar{b}$  asymmetry. Improved experimental precision may strengthen the relevance of these EWPOs in order to constrain supersymmetry-inspired models in the future (and possibly discriminate among them), reducing both the experimental uncertainty and the theoretical parametric error. Yet much effort will then be necessary to reduce the higher-order uncertainty and thus achieve theoretical results of comparable accuracy.

## Acknowledgements

The authors acknowledge discussions with S. Heinemeyer and G. Weiglein and also wish to thank U. Ellwanger and U. Nierste for useful discussions and comments. The work of F.D. was supported by the EU Contract No. MRTN-CT-2006-035482, FLAVIANet, by DFG through project C6 of the collective research centre SFB-TR9 and by BMBF grant 05H09VKF.

## References

- [1] D. Y. Bardin *et al.*, CERN-95-03A, CERN-YELLOW-95-03A, Sep 1997. arXiv:hep-ph/9709229.  
D. Y. Bardin, M. Grunewald and G. Passarino, arXiv:hep-ph/9902452.
- [2] [ALEPH, DELPHI, L3, OPAL, SLD Collaborations, LEP Electroweak Working Group, SLD Electroweak and Heavy Flavour Groups], Phys. Rept. **427**, 257 (2006)  
[ALEPH, DELPHI, L3, OPAL Collaborations, LEP Electroweak Working Group], arXiv:hep-ex/0511027.  
webpage: lepewwg.web.cern.ch/LEPEWWG/Welcome.html
- [3] [Tevatron Electroweak Working Group and CDF and D0 Collaboration], arXiv:0908.1374 [hep-ex].  
webpage: tevewwg.fnal.gov
- [4] N. Besson, M. Boonekamp, E. Klinkby, T. Petersen and S. Mehlhase [ATLAS Collaboration], Eur. Phys. J. C **57**, 627 (2008) [arXiv:0805.2093 [hep-ex]].
- [5] S. Heinemeyer and G. Weiglein, arXiv:1007.5232 [hep-ph].
- [6] M. W. Grunewald, J. Phys. Conf. Ser. **110**, 042008 (2008) [arXiv:0709.3744 [hep-ph]].  
M. W. Grunewald, arXiv:0710.2838 [hep-ex].
- [7] [ALEPH, DELPHI, L3, OPAL Collaborations, LEP Working Group for Higgs boson searches], Phys. Lett. B **565** (2003) 61 [arXiv:hep-ex/0306033].
- [8] S. Heinemeyer, W. Hollik and G. Weiglein, Phys. Rept. **425** (2006) 265 [arXiv:hep-ph/0412214].
- [9] S. Heinemeyer, W. Hollik, D. Stockinger, A. M. Weber and G. Weiglein, JHEP **0608** (2006) 052 [arXiv:hep-ph/0604147].
- [10] S. Heinemeyer, W. Hollik, A. M. Weber and G. Weiglein, JHEP **0804** (2008) 039 [arXiv:0710.2972 [hep-ph]].
- [11] J. R. Ellis, S. Heinemeyer, K. A. Olive and G. Weiglein, JHEP **0502** (2005) 013 [arXiv:hep-ph/0411216].  
J. R. Ellis, S. Heinemeyer, K. A. Olive and G. Weiglein, JHEP **0605** (2006) 005 [arXiv:hep-ph/0602220].  
J. R. Ellis, S. Heinemeyer, K. A. Olive, A. M. Weber and G. Weiglein, JHEP **0708** (2007) 083 [arXiv:0706.0652 [hep-ph]].  
B. C. Allanach, C. G. Lester and A. M. Weber, JHEP **0612** (2006) 065 [arXiv:hep-ph/0609295].  
B. C. Allanach, K. Cranmer, C. G. Lester and A. M. Weber, JHEP **0708** (2007) 023 [arXiv:0705.0487 [hep-ph]].  
L. Roszkowski, R. R. de Austri and R. Trotta, JHEP **0704** (2007) 084 [arXiv:hep-ph/0611173].  
O. Buchmueller *et al.*, Phys. Lett. B **657** (2007) 87 [arXiv:0707.3447 [hep-ph]].
- [12] [ALEPH, DELPHI, L3, OPAL Collaborations, LEP Working Group for Higgs boson searches], Eur. Phys. J. C **47** (2006) 547 [arXiv:hep-ex/0602042].
- [13] U. Ellwanger, C. Hugonie and A. M. Teixeira, arXiv:0910.1785 [hep-ph]. (*and ref. therein*)

- [14] J. E. Kim and H. P. Nilles, *Phys. Lett. B* **138** (1984) 150.
- [15] U. Ellwanger and C. Hugonie, *Eur. Phys. J. C* **25** (2002) 297 [arXiv:hep-ph/9909260].
- [16] R. Dermisek and J. F. Gunion, *Phys. Rev. Lett.* **95** (2005) 041801 [arXiv:hep-ph/0502105].
- [17] [ALEPH Collaboration], *JHEP* **1005** (2010) 049 [arXiv:1003.0705 [hep-ex]].
- [18] R. Dermisek and J. F. Gunion, *Phys. Rev. D* **81**, 075003 (2010) [arXiv:1002.1971 [hep-ph]].
- [19] R. Dermisek and J. F. Gunion, *Phys. Rev. D* **73** (2006) 111701 [arXiv:hep-ph/0510322].
- [20] J. Cao and J. M. Yang, *JHEP* **0812** (2008) 006 [arXiv:0810.0751 [hep-ph]].
- [21] J. Cao, Z. Heng and J. M. Yang, arXiv:1007.1918 [hep-ph].
- [22] A. Sirlin, *Phys. Rev. D* **22** (1980) 971.  
W. J. Marciano and A. Sirlin, *Phys. Rev. D* **22** (1980) 2695 [Erratum-ibid. *D* **31** (1985) PHRVA,D31,213.1985) 213].
- [23] A. Djouadi and C. Verzegnassi, *Phys. Lett. B* **195** (1987) 265.  
A. Djouadi, *Nuovo Cim. A* **100** (1988) 357.  
B. A. Kniehl, *Nucl. Phys. B* **347** (1990) 86.  
F. Halzen and B. A. Kniehl, *Nucl. Phys. B* **353** (1991) 567.  
B. A. Kniehl and A. Sirlin, *Nucl. Phys. B* **371** (1992) 141.  
B. A. Kniehl and A. Sirlin, *Phys. Rev. D* **47** (1993) 883.  
A. Djouadi and P. Gambino, *Phys. Rev. D* **49** (1994) 3499 [Erratum-ibid. *D* **53** (1996) 4111] [arXiv:hep-ph/9309298].  
A. Freitas, W. Hollik, W. Walter and G. Weiglein, *Phys. Lett. B* **495** (2000) 338 [Erratum-ibid. *B* **570** (2003) 260] [arXiv:hep-ph/0007091].  
A. Freitas, W. Hollik, W. Walter and G. Weiglein, *Nucl. Phys. B* **632** (2002) 189 [Erratum-ibid. *B* **666** (2003) 305] [arXiv:hep-ph/0202131].  
M. Awramik and M. Czakon, *Phys. Lett. B* **568** (2003) 48 [arXiv:hep-ph/0305248].  
M. Awramik and M. Czakon, *Phys. Rev. Lett.* **89** (2002) 241801 [arXiv:hep-ph/0208113].  
A. Onishchenko and O. Veretin, *Phys. Lett. B* **551** (2003) 111 [arXiv:hep-ph/0209010].  
M. Awramik, M. Czakon, A. Onishchenko and O. Veretin, *Phys. Rev. D* **68** (2003) 053004 [arXiv:hep-ph/0209084].
- [24] M. Awramik, M. Czakon, A. Freitas and G. Weiglein, *Phys. Rev. D* **69** (2004) 053006 [arXiv:hep-ph/0311148].
- [25] L. Avdeev, J. Fleischer, S. Mikhailov and O. Tarasov, *Phys. Lett. B* **336** (1994) 560 [Erratum-ibid. *B* **349** (1995) 597] [arXiv:hep-ph/9406363].  
K. G. Chetyrkin, J. H. Kuhn and M. Steinhauser, *Phys. Lett. B* **351** (1995) 331 [arXiv:hep-ph/9502291].  
K. G. Chetyrkin, J. H. Kuhn and M. Steinhauser, *Phys. Rev. Lett.* **75** (1995) 3394 [arXiv:hep-ph/9504413].  
J. J. van der Bij, K. G. Chetyrkin, M. Faisst, G. Jikia and T. Seidensticker, *Phys. Lett. B* **498** (2001) 156 [arXiv:hep-ph/0011373].  
R. Boughezal, J. B. Tausk and J. J. van der Bij, *Nucl. Phys. B* **713** (2005) 278 [arXiv:hep-ph/0410216].  
M. Faisst, J. H. Kuhn, T. Seidensticker and O. Veretin, *Nucl. Phys. B* **665** (2003) 649 [arXiv:hep-ph/0302275].

- Y. Schroder and M. Steinhauser, Phys. Lett. B **622** (2005) 124 [arXiv:hep-ph/0504055].
- K. G. Chetyrkin, M. Faisst, J. H. Kuhn, P. Maierhofer and C. Sturm, Phys. Rev. Lett. **97** (2006) 102003 [arXiv:hep-ph/0605201].
- R. Boughezal and M. Czakon, Nucl. Phys. B **755** (2006) 221 [arXiv:hep-ph/0606232].
- [26] G. Montagna, O. Nicrosini, F. Piccinini and G. Passarino, Comput. Phys. Commun. **117** (1999) 278 [arXiv:hep-ph/9804211].
- [27] D. Y. Bardin, P. Christova, M. Jack, L. Kalinovskaya, A. Olchevski, S. Riemann and T. Riemann, Comput. Phys. Commun. **133** (2001) 229 [arXiv:hep-ph/9908433].
- [28] A. B. Arbuzov *et al.*, Comput. Phys. Commun. **174** (2006) 728 [arXiv:hep-ph/0507146].
- [29] H. Flacher, M. Goebel, J. Haller, A. Hocker, K. Monig and J. Stelzer, Eur. Phys. J. C **60** (2009) 543 [arXiv:0811.0009 [hep-ph]].
- [30] K. Nakamura *et al.* [Particle Data Group], J. Phys. G **37**, 075021 (2010)
- [31] G. Degrossi and P. Gambino, Nucl. Phys. B **567** (2000) 3 [arXiv:hep-ph/9905472].
- M. Awramik, M. Czakon, A. Freitas and G. Weiglein, Phys. Rev. Lett. **93** (2004) 201805 [arXiv:hep-ph/0407317].
- W. Hollik, U. Meier and S. Uccirati, Nucl. Phys. B **731** (2005) 213 [arXiv:hep-ph/0507158].
- W. Hollik, U. Meier and S. Uccirati, Phys. Lett. B **632** (2006) 680 [arXiv:hep-ph/0509302].
- W. Hollik, U. Meier and S. Uccirati, Nucl. Phys. B **765** (2007) 154 [arXiv:hep-ph/0610312].
- M. Awramik, M. Czakon and A. Freitas, Phys. Lett. B **642** (2006) 563 [arXiv:hep-ph/0605339].
- M. Awramik, M. Czakon and A. Freitas, JHEP **0611** (2006) 048 [arXiv:hep-ph/0608099].
- [32] R. Barbieri and L. Maiani, Nucl. Phys. B **224** (1983) 32.
- C. S. Lim, T. Inami and N. Sakai, Phys. Rev. D **29** (1984) 1488.
- E. Eliasson, Phys. Lett. B **147** (1984) 65.
- Z. Hioki, Prog. Theor. Phys. **73** (1985) 1283.
- J. A. Grifols and J. Sola, Nucl. Phys. B **253** (1985) 47.
- R. Barbieri, M. Frigeni, F. Giuliani and H. E. Haber, Nucl. Phys. B **341** (1990) 309.
- M. Drees and K. Hagiwara, Phys. Rev. D **42** (1990) 1709.
- M. Drees, K. Hagiwara and A. Yamada, Phys. Rev. D **45** (1992) 1725.
- P. H. Chankowski, A. Dabelstein, W. Hollik, W. M. Mosle, S. Pokorski and J. Rosiek, Nucl. Phys. B **417** (1994) 101.
- D. Garcia and J. Sola, Mod. Phys. Lett. A **9** (1994) 211.
- D. M. Pierce, J. A. Bagger, K. T. Matchev and R. j. Zhang, Nucl. Phys. B **491** (1997) 3 [arXiv:hep-ph/9606211].
- [33] S. Heinemeyer, W. Hollik, F. Merz and S. Penaranda, Eur. Phys. J. C **37** (2004) 481 [arXiv:hep-ph/0403228].
- [34] S. K. Kang and J. D. Kim, Phys. Rev. D **62** (2000) 071901 [arXiv:hep-ph/0008073].
- [35] M. Consoli, W. Hollik and F. Jegerlehner, Phys. Lett. B **227** (1989) 167.
- [36] A. Djouadi, P. Gambino, S. Heinemeyer, W. Hollik, C. Junger and G. Weiglein, Phys. Rev. Lett. **78** (1997) 3626 [arXiv:hep-ph/9612363].
- A. Djouadi, P. Gambino, S. Heinemeyer, W. Hollik, C. Junger and G. Weiglein, Phys. Rev. D **57** (1998) 4179 [arXiv:hep-ph/9710438].

- [37] S. Heinemeyer and G. Weiglein, *JHEP* **0210** (2002) 072 [arXiv:hep-ph/0209305].  
J. Haestier, S. Heinemeyer, D. Stockinger and G. Weiglein, *JHEP* **0512** (2005) 027 [arXiv:hep-ph/0508139].
- [38] S. Marchetti, S. Mertens, U. Nierste and D. Stockinger, *Phys. Rev. D* **79** (2009) 013010 [arXiv:0808.1530 [hep-ph]].
- [39] U. Ellwanger, J. F. Gunion and C. Hugonie, *JHEP* **0502** (2005) 066 [arXiv:hep-ph/0406215].  
U. Ellwanger and C. Hugonie, *Comput. Phys. Commun.* **175** (2006) 290 [arXiv:hep-ph/0508022].  
webpage: <http://www.th.u-psud.fr/NMHDECAY/nmssmtools.html>
- [40] F. Domingo and U. Ellwanger, *JHEP* **0712**, 090 (2007) [arXiv:0710.3714 [hep-ph]].
- [41] F. Domingo, U. Ellwanger, E. Fullana, C. Hugonie and M. A. Sanchis-Lozano, *JHEP* **0901** (2009) 061 [arXiv:0810.4736 [hep-ph]]  
F. Domingo, arXiv:1010.4701 [hep-ph].
- [42] F. Domingo and U. Ellwanger, *JHEP* **0807** (2008) 079 [arXiv:0806.0733 [hep-ph]].
- [43] M. Davier, A. Hoecker, B. Malaescu and Z. Zhang, arXiv:1010.4180 [hep-ph].
- [44] S. Andreas, O. Lebedev, S. Ramos-Sanchez and A. Ringwald, arXiv:1005.3978 [hep-ph].

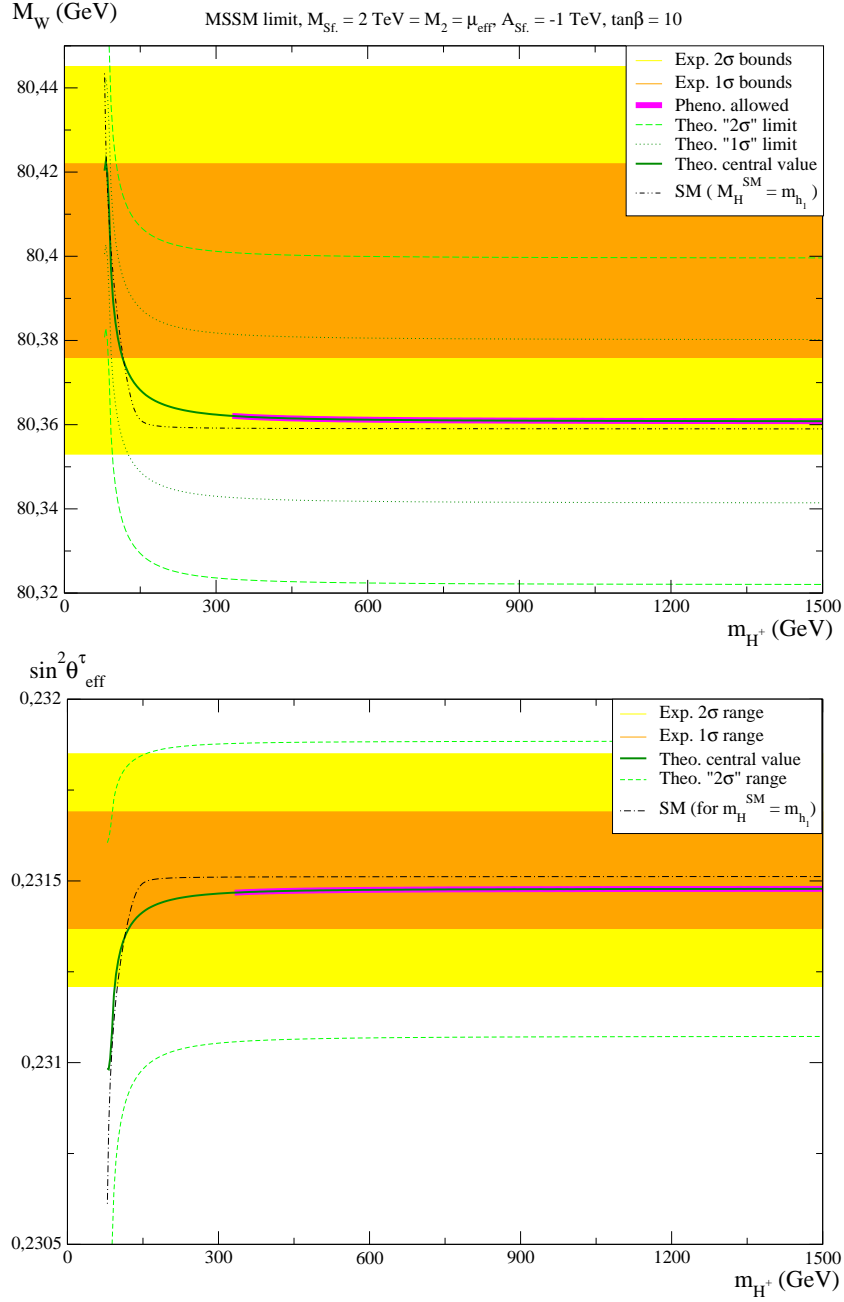


Figure 1: Impact of the Higgs sector on  $M_W$  and  $\sin^2 \theta_{\text{eff}}^\tau$ , in the MSSM limit. Supersymmetric effects are suppressed by the choice of a heavy SUSY scale  $\sim 2 \text{ TeV}$ . Here and below, the experimental  $1\sigma$  and  $2\sigma$  ranges are depicted in orange and yellow, respectively. The dark-green curve corresponds to the theoretical prediction, flanked by its light-green dashed uncertainty limits (the dotted dark-green curves in the case of the  $M_W$  plot correspond to a “ $1\sigma$ ” half-error). The SM contribution, for a SM Higgs mass equal to the lightest MSSM-like CP-even Higgs state ( $M_H^{\text{SM}} = m_{h_1^0}$ ; note that, on the “plateau” when  $m_{H^\pm} \geq 250 \text{ GeV}$ ,  $m_{h_1^0} \sim 117 \text{ GeV}$ ) is represented by the dot-dash black curves. The “pink aura” around the dark-green curve corresponds to points which were found in agreement with all constraints implemented in NMSSMTools: the lower mass-range is excluded by LEP constraints on Higgs searches.

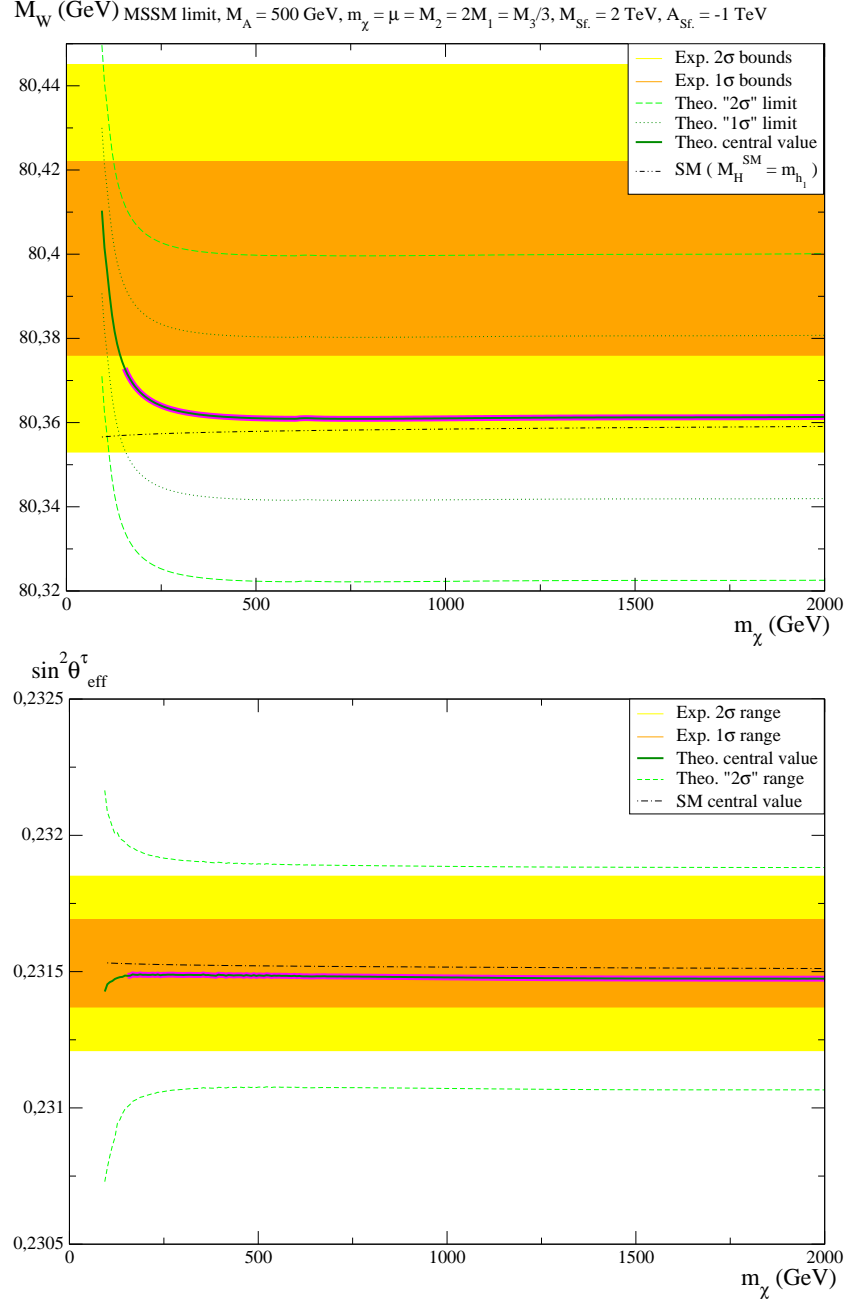


Figure 2: Impact of the gaugino-higgsino sector on  $M_W$  and  $\sin^2 \theta_{\text{eff}}^\tau$  in the MSSM limit. A common scale  $m_\chi \equiv \mu_{\text{eff}} = M_2 = 2M_1 = M_3/3$  was used for the scan. Here and below, the heavy Higgs doublet is set at a scale  $\sim 500$  GeV. The Sfermion sector is still very heavy ( $\sim 2$  TeV). The colour-code is similar to that of Fig. 1. The lower mass range is excluded by the experimental lower-bounds on chargino/neutralino masses.



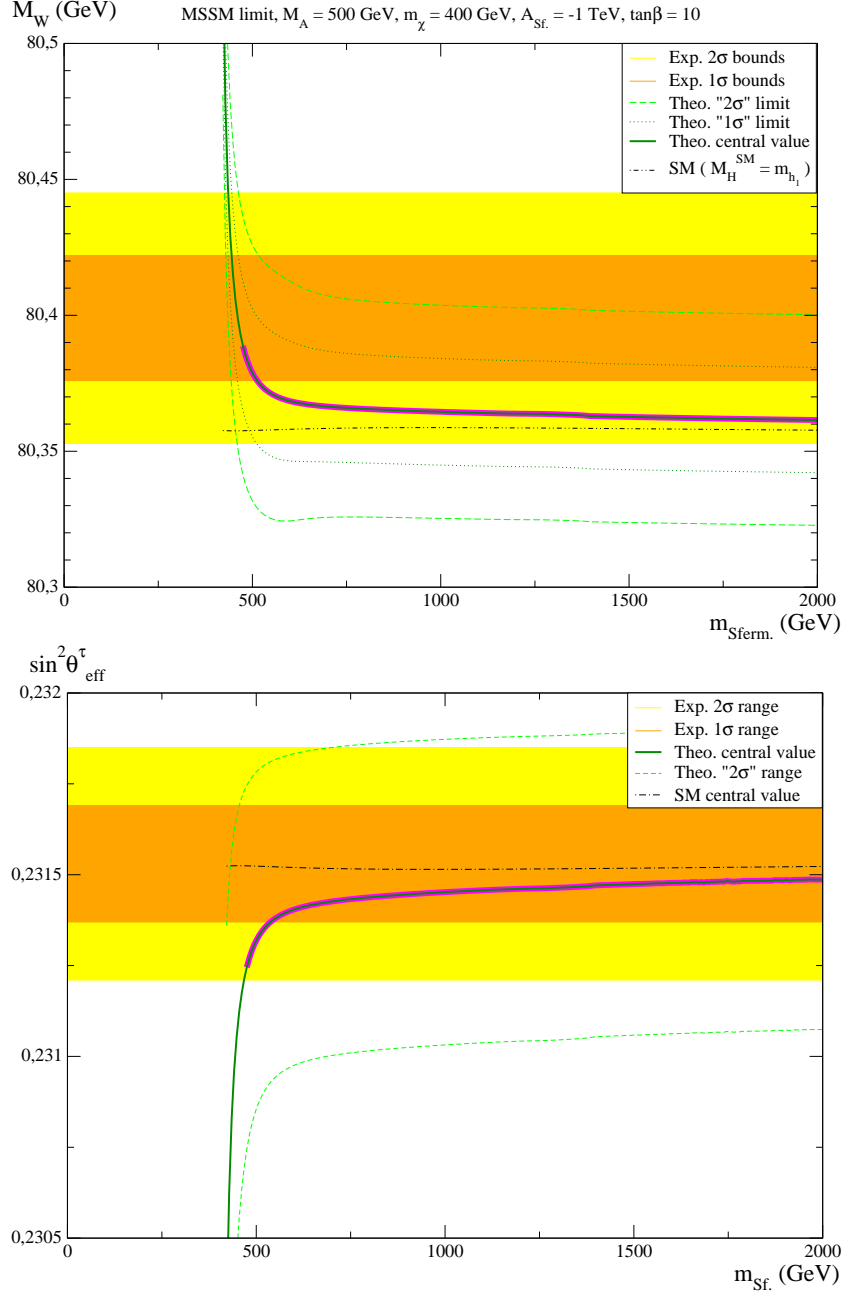


Figure 3: Impact of the sfermions on  $M_W$ ,  $\sin^2 \theta_{\text{eff}}^\tau$  in the MSSM limit. The scan was performed over a universal soft SUSY-breaking sfermion mass  $m_{\text{sf.}}$ , the trilinear couplings remaining at  $-1$  TeV (Therefore, the stop sector always provides the lightest and the heaviest sfermion. Note that the sfermion contribution to the lightest Higgs mass remains sufficient to circumvent LEP bounds, essentially due to heavy states, with mass over 500 GeV).  $m_\chi \equiv \mu_{\text{eff}} = M_2 = 2M_1 = M_3/3 = 400$  GeV. The colour-code remains as in Fig. 1. Constraints on the masses of sfermion states exclude the lower mass-range.

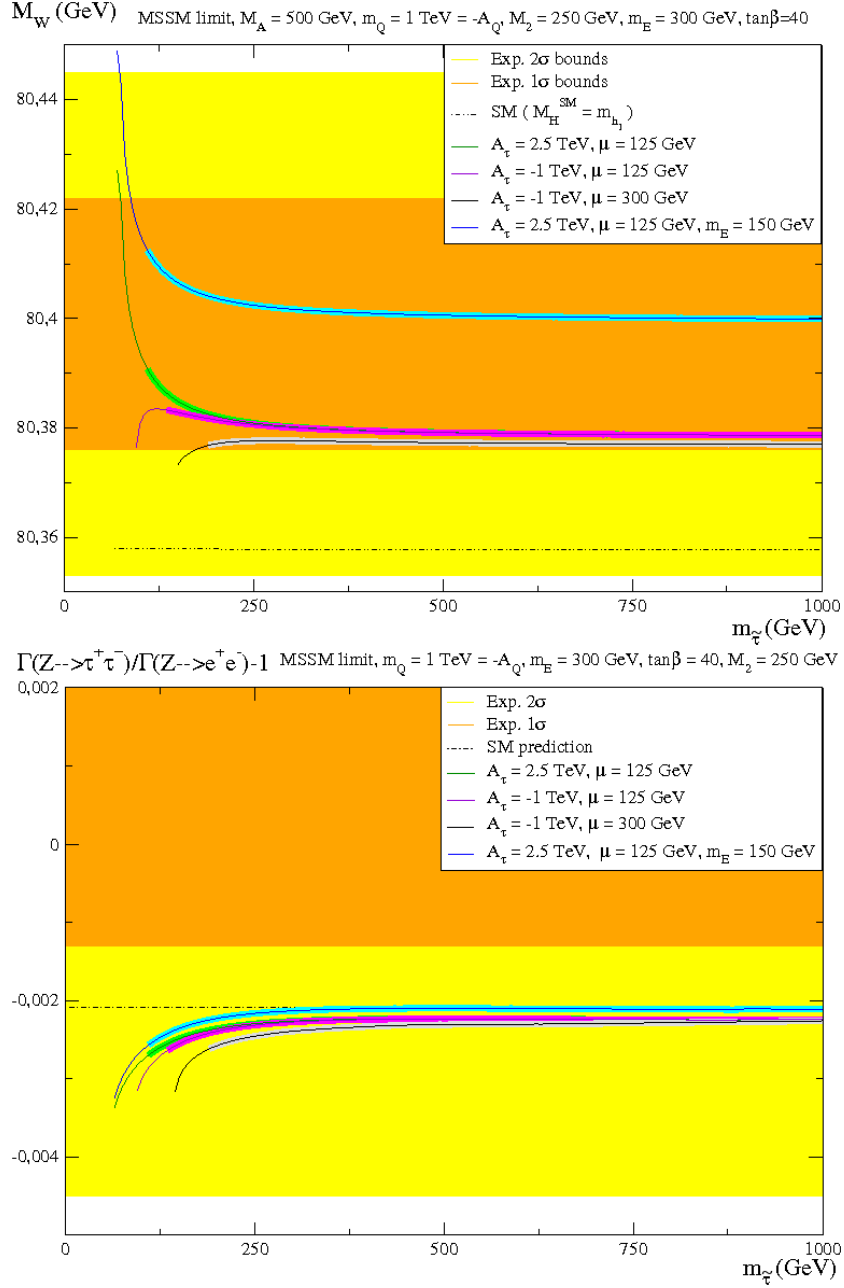


Figure 4: Impact of the slepton sector on  $M_W$  and  $\Gamma(Z \rightarrow \tau^+\tau^-)/\Gamma(Z \rightarrow e^+e^-) - 1$  in the MSSM limit. The scan was performed over a soft SUSY-breaking (left- and right-) stau mass  $m_{\tilde{\tau}}$ , for several values of  $\mu_{\text{eff}}$  and the trilinear coupling  $A_\tau$ , in order to vary the stau mixing:  $(A_\tau, \mu_{\text{eff}})$  is chosen as (2.5 TeV, 125 GeV) for the green curve (small mixing), (-1 TeV, 125 GeV) for the violet curve, (-1 TeV, 300 GeV) for the black curve (large mixing). The sleptons of the first two generations have a soft mass of  $m_{\tilde{E}} = 300$  GeV. The blue curve is similar to the green one, but for  $m_{\tilde{E}} = 150$  GeV. As before, the “auras” alongside the curves correspond to points passing the constraints of NMSSMTools (the lower mass-range being excluded by bounds on slepton masses). The theoretical error bars are not displayed, but the uncertainty is similar in magnitude to that of *e.g.* Fig 1.

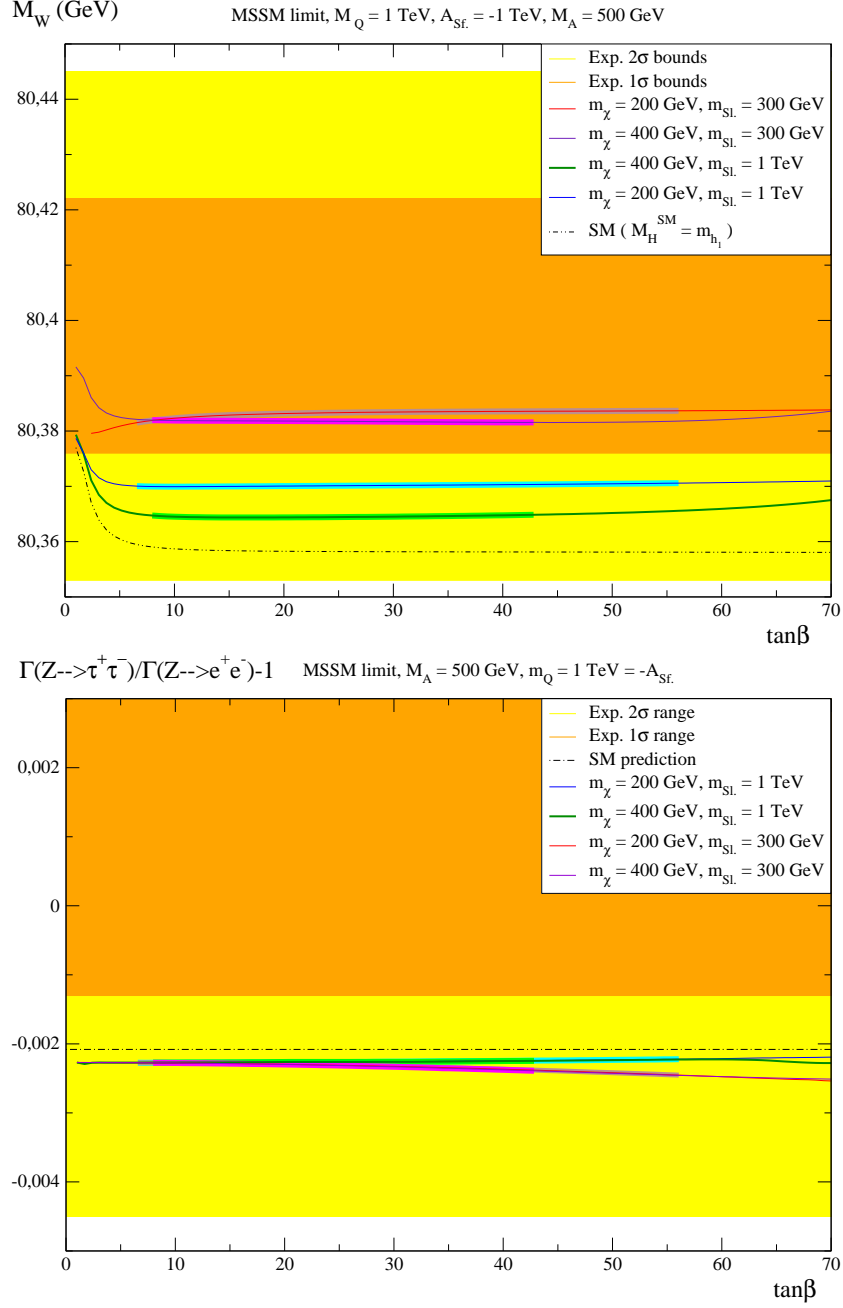


Figure 5: Impact of  $\tan\beta$  on  $M_W$  and  $\Gamma(Z \rightarrow \tau^+\tau^-)/\Gamma(Z \rightarrow e^+e^-) - 1$  in the MSSM limit. The scan was performed for several slepton and chargino/neutralino scales:  $(m_\chi, m_{\tilde{E},\tilde{\tau}}) = (400 \text{ GeV}, 1 \text{ TeV})$  for the green curve,  $(200 \text{ GeV}, 1 \text{ TeV})$ ,  $(400 \text{ GeV}, 300 \text{ GeV})$  and  $(200 \text{ GeV}, 300 \text{ GeV})$  respectively for the blue, violet and red ones. Constraints applying at low  $\tan\beta$  originate from bounds on the lightest Higgs mass, while the large  $\tan\beta$  regime is excluded by  $B$ -physics processes ( $BR(\bar{B}_s^0 \rightarrow \mu^+\mu^-)$ ).

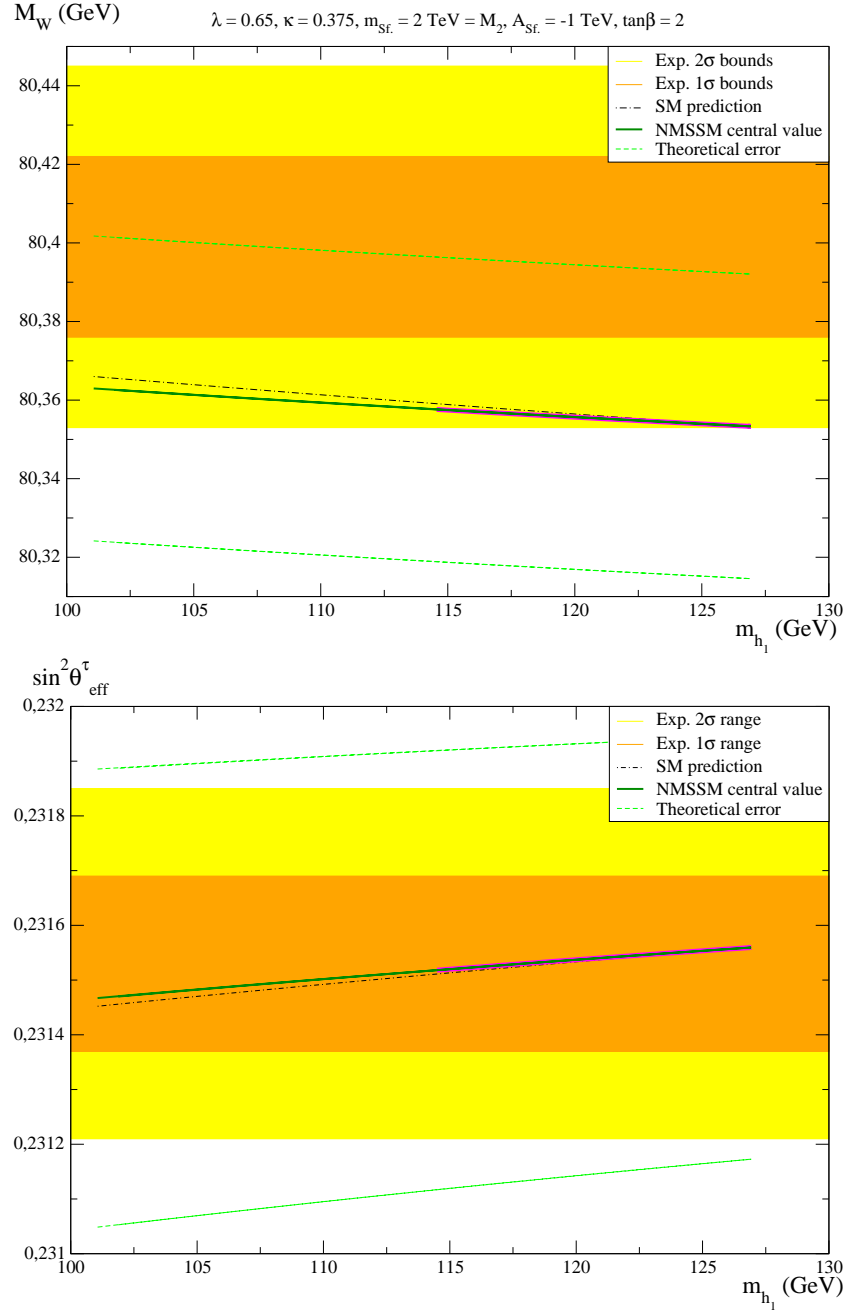


Figure 6: NMSSM prediction for  $M_W$  and  $\sin^2 \theta_{\text{eff}}^\tau$  in the low  $\tan \beta$  regime ( $\tan \beta = 2$ ). The supersymmetric sector was chosen heavy ( $\sim 2 \text{ TeV}$ ), in order to highlight Higgs effects. The colour-code is similar to *e.g.* Fig. 1.

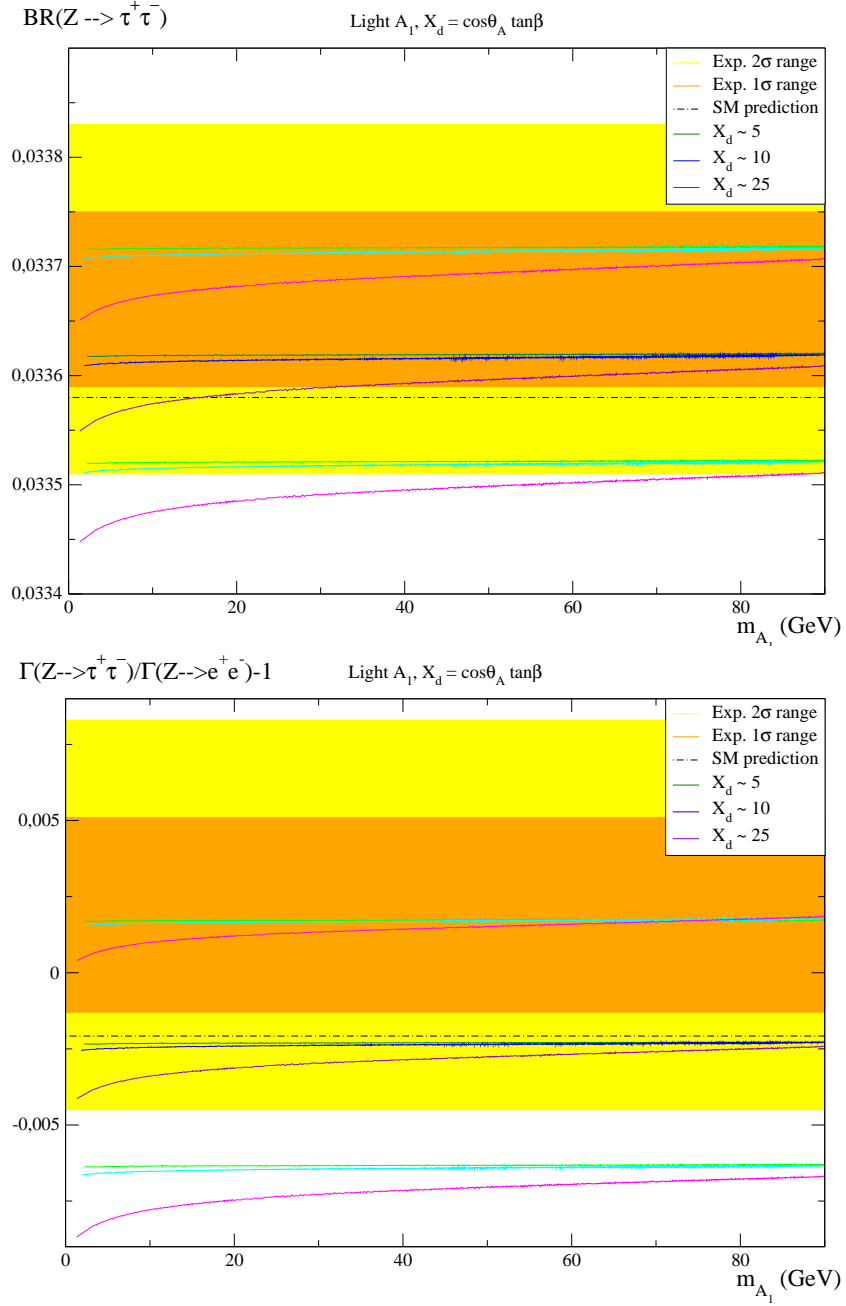


Figure 7: Impact of the NMSSM light CP-odd Higgs  $BR(Z \rightarrow \tau^+ \tau^-)$  and  $\Gamma(Z \rightarrow \tau^+ \tau^-) / \Gamma(Z \rightarrow e^+ e^-) - 1$ . Sfermion effects are suppressed by the choice of a heavy scale  $\sim 2$  TeV. The reduced coupling of the light CP-odd Higgs  $X_d \equiv \cos\theta_A \tan\beta$  is maintained constant ( $\pm 0.3$ ) at 5 (dark green curve), 10 (dark blue curve) and 25 (violet curve). The theoretical uncertainty is bounded by the paler (green, blue and pink) curves. Corresponding effects on  $M_W$  and  $\sin^2 \theta_{\text{eff}}^\tau$  were found negligible.

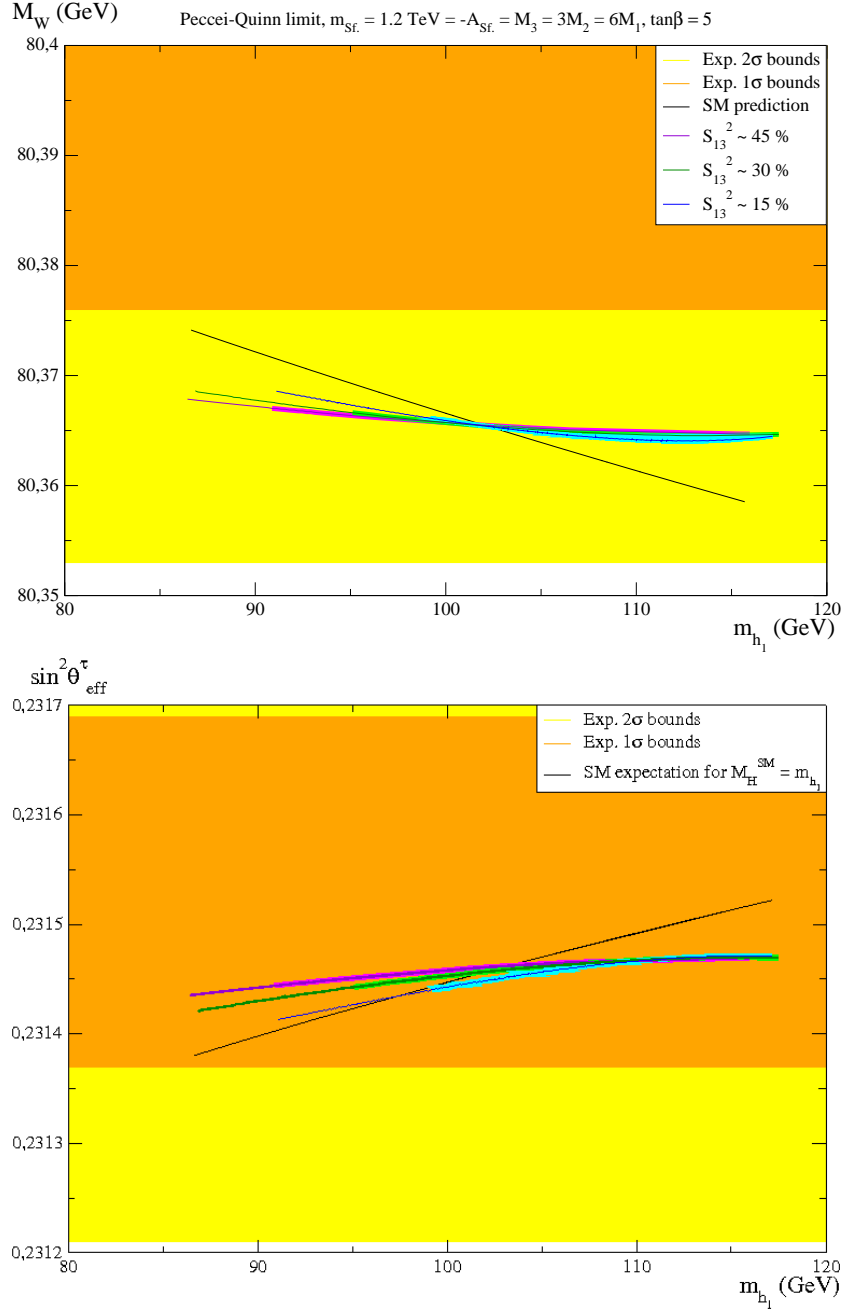


Figure 8: Impact of the light doublet-like CP-even Higgs (in an approximate Peccei-Quinn limit  $\frac{\kappa}{\lambda} = 0.1$ , with  $\lambda = 0.5$ ) on  $M_W$  and  $\sin^2 \theta_{\text{eff}}^\tau$ . As explained in the main part of the text, the light CP-even Higgs  $h_1$  possesses a significant subdominant singlet component:  $\sim 45\%$ ,  $\sim 30\%$  and  $\sim 15\%$  respectively for the violet, blue and green curves. The lighter “aura” indicates as before points which were found in agreement with all constraints implemented in NMSSMTools, included the recent ALEPH constraints. These latter limits are those relevant for the lower  $h_1$  mass range. Note that the “SM expectation for  $M_H^{\text{SM}} = m_{h_1}$ ” is shown to allow for the comparison, but corresponds to Higgs masses which, in the SM, contrary to the NMSSM, are phenomenologically excluded.

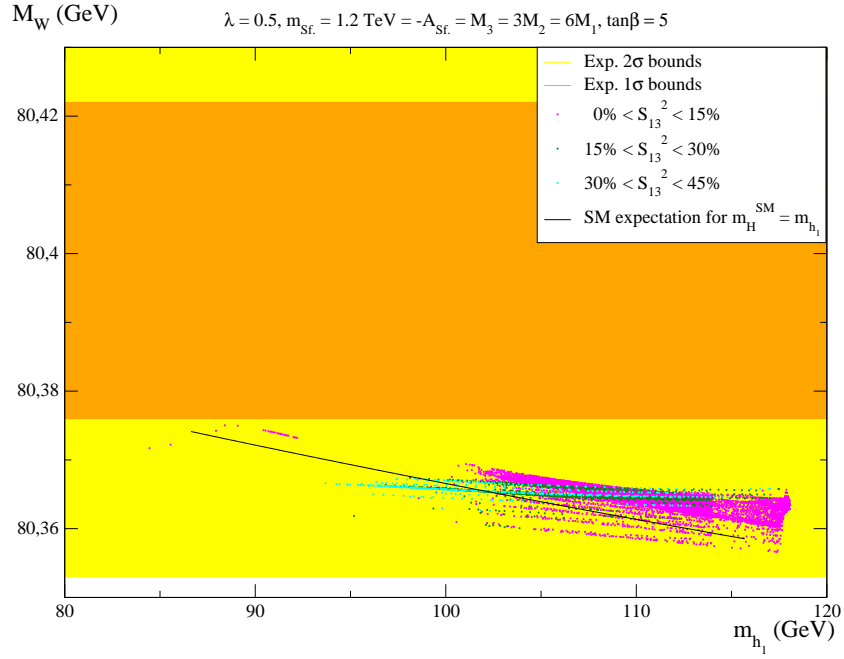


Figure 9: Impact of the light doublet-like CP-even Higgs (with  $\lambda = 0.5$ ,  $\tan\beta = 5$ ) on  $M_W$ . This scatter plot is obtained by scanning over the parameters  $A_\lambda$ ,  $A_\kappa$ ,  $\mu_{\text{eff}}$  and  $\kappa$  (with the requirement that  $m_{A_1} = 9\text{--}10 \text{ GeV}$ ) and retaining all the points allowed by the phenomenological constraints implemented in NMSSMTools.

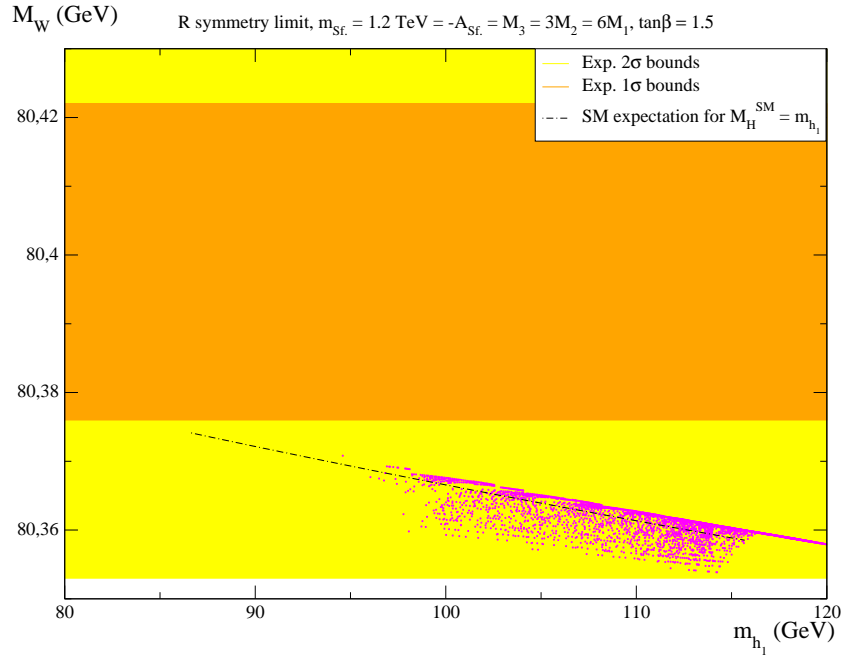


Figure 10: Impact of the light doublet-like CP-even Higgs (with  $\lambda = 0.5$ ,  $\tan\beta = 1.5$ ) on  $M_W$ . This scatter plot is obtained by scanning over the parameters  $A_\lambda$ ,  $A_\kappa$  ( $|A_{\lambda,\kappa}| < 50 \text{ GeV}$  to ensure an approximate R-symmetry),  $\mu_{\text{eff}}$  and  $\kappa$  (with the requirement that  $m_{A_1} = 9\text{--}10 \text{ GeV}$ ) and retaining all the points allowed by the phenomenological constraints implemented in NMSSMTools.

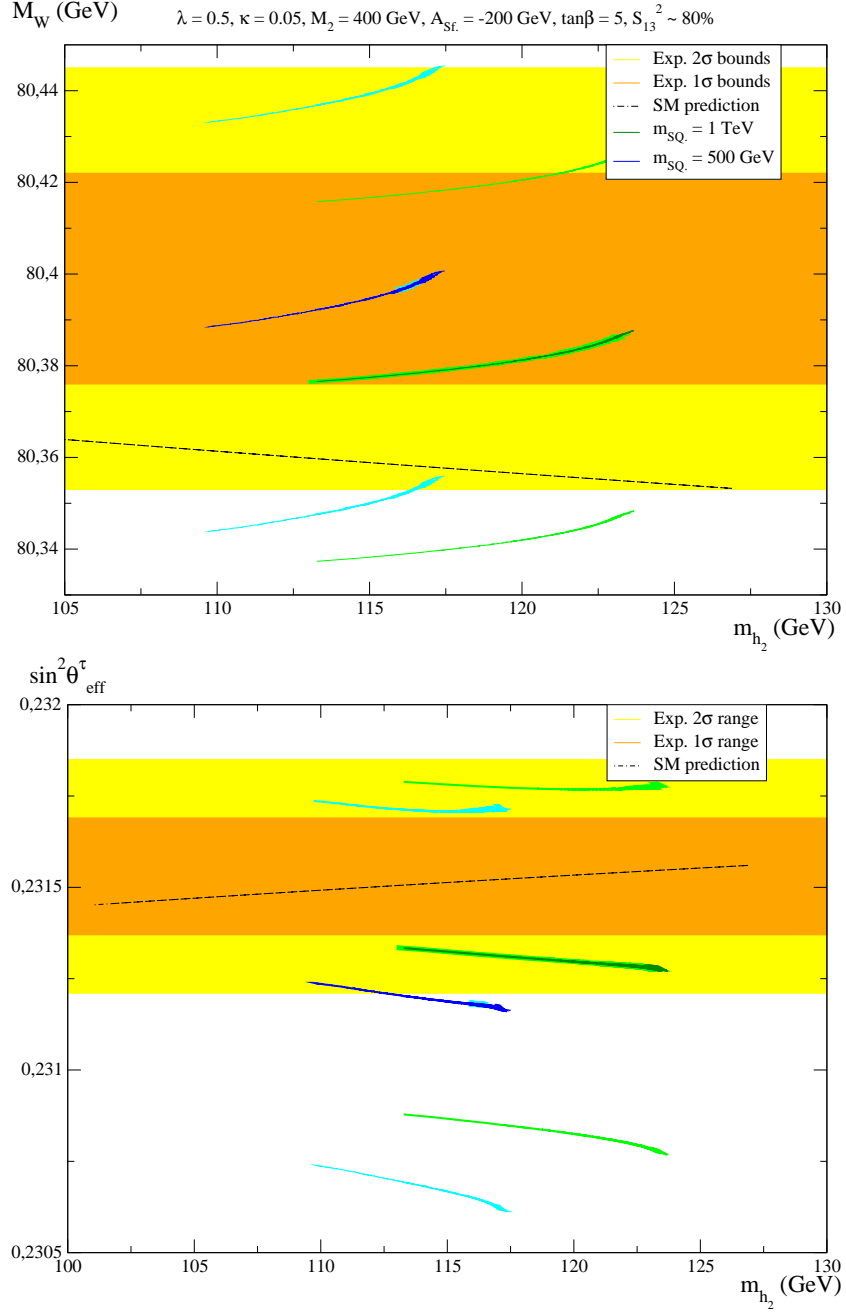


Figure 11: Light singlet-like CP-even Higgs scenario (in an approximate Peccei-Quinn limit  $\frac{\kappa}{\lambda} = 0.1$ , with  $\lambda = 0.5$ ):  $M_W$  and  $\sin^2 \theta_{\text{eff}}^\tau$  are plotted against the mass of the observable doublet-like state  $m_{h_2}$ , for  $S_{13}^2 \sim 0.8 (\pm 0.002)$  (note that the corresponding  $h_1$  masses, for the allowed points, are in the range  $\sim [40, 110]$  GeV). The dark-green and dark-blue curves correspond to the theoretical central values for universal squark soft-masses of respectively 1 TeV and 500 GeV (The lighter “aura” indicates points which were found in agreement with all constraints implemented in NMSSMTools). The error bars are displayed in light-green and light-blue respectively.



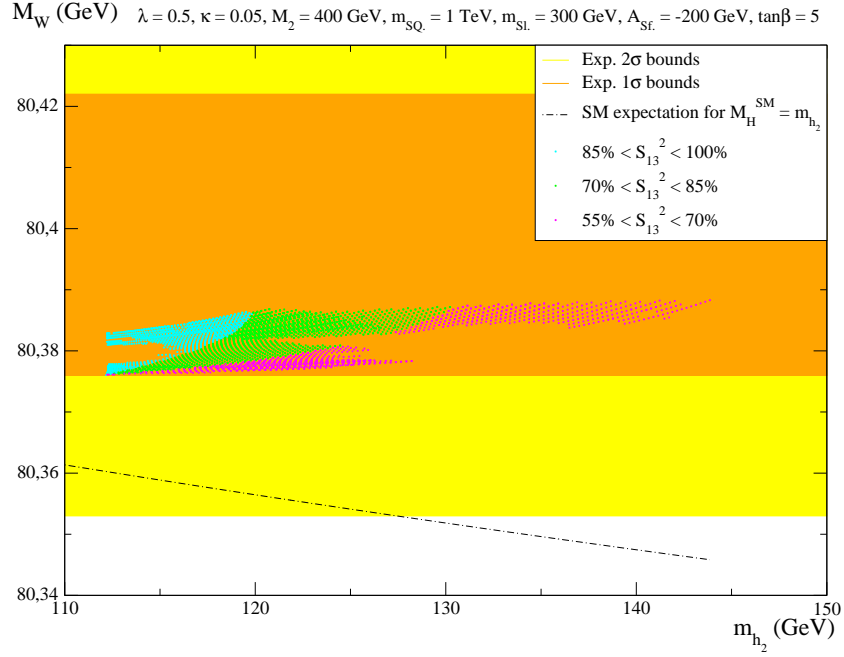


Figure 12: Light singlet-like CP-even Higgs scenario (in an approximate Peccei-Quinn limit  $\frac{\kappa}{\lambda} = 0.1$ , with  $\lambda = 0.5$ ): scatter plot for  $M_W$  against the mass of the observable doublet-like state  $m_{h_2}$ . Squarks are taken at a heavy scale  $m_{\tilde{Q}} = 1 \text{ TeV}$ , while, for sleptons,  $m_{\text{sl}} = 300 \text{ GeV}$ . Light blue, green and pink points satisfy the constraints implemented in NMSSMTools and verify respectively  $S_{13}^2 \in [0.85, 1]$ ,  $\in [0.7, 0.85]$ ,  $\in [0.55, 0.7]$ . Corresponding  $h_1$  masses are in the range  $[40, 110] \text{ GeV}$ . The dot-dash black curve shows the expected SM central value for a SM Higgs of similar mass. The “cuts” inside the allowed regions are essentially related to LEP limits on Higgs production.